View this PDF in Utopia Documents for more interactive functionality
Download FREE software now

Biochem. J. (2014) **457**, 379–390 (Printed in Great Britain) doi:10.1042/BJ20130413

online data

Secret of the major birch pollen allergen Bet v 1: identification of the physiological ligand

Christian SEUTTER VON LOETZEN*, Thomas HOFFMANN†, Maximilian J. HARTL*, Kristian SCHWEIMER*, Wilfried SCHWAB†, Paul RÖSCH* and Olivia HARTL-SPIEGELHAUER*[1]

*Lehrstuhl Biopolymere und Forschungszentrum für Bio-Makromoleküle, Universität Bayreuth, Universitätsstr. 30, 95447 Bayreuth, Germany
†Biotechnology of Natural Products, Technische Universität München, Liesel-Beckmann-Str. 1, 85354 Freising, Germany

The major birch pollen allergen Bet v 1 is the main elicitor of airborne type I allergies and belongs to the PR-10 family (pathogenesis-related proteins 10). Bet v 1 is the most extensively studied allergen, and is well characterized at a biochemical and immunological level; however, its physiological function remains elusive. In the present study, we identify Q3OS (quercetin-3-*O*-sophoroside) as the natural ligand of Bet v 1. We isolated Q3OS bound to Bet v 1 from mature birch pollen and confirmed its binding by reconstitution of the Bet v 1–Q3OS complex. Fluorescence and UV–visible spectroscopy experiments, as well as HSQC (heteronuclear single-quantum coherence) titration, and the comparison with model compounds, such as quercetin, indicated the specificity of Q3OS binding. Elucidation of the binding site by NMR combined with a computational model resulted in a more detailed understanding and shed light on the physiological function of Bet v 1. We postulate that the binding of Q3OS to Bet v 1 plays an important, but as yet unclear, role during the inflammation response and Bet v 1 recognition by IgE.

Key words: allergen, Bet v 1, NMR, quercetin-3-*O*-sophoroside (Q3OS).

INTRODUCTION

The major birch pollen allergen Bet v 1 from *Betula verrucosa* (European white birch) [1] probably exceeds 20 % (w/w) of the total protein content of mature pollen and is an elicitor of airborne type I allergies [2,3]. Up to 20 % of the population of the temperate climate zone of the northern hemisphere are affected by pollen allergies, and 50–90 % of these patients are sensitized to Bet v 1 [4–7]. Up to 90 % of the latter individuals also exhibit IgE-mediated allergic cross-reactions (oral allergy syndrome) to Bet v 1 homologous food allergens contained in fruits, vegetables and nuts [8,9].

On the basis of amino acid sequence similarities and the protein 3D structures, Bet v 1 as well as homologous pollen and food allergens belong to the plant PR-10 proteins (pathogenesis-related proteins 10) family within the Bet-v-1-like superfamily. The PR-10 family is ubiquitous in Nature, and proteins of this family can be found in virtually all plants studied [10]. They are part of the immune defence mostly induced by microbial attacks [11,12], fungal elicitors [13,14], wounds [15] or abiotic stress stimuli [16]. Additionally, they are expressed constitutively in different plant compartments during various developmental stages. PR-10 family proteins are encoded by multiple genes and thus occur as a mixture of different isoforms [17]. Although several PR-10 proteins are well characterized, their particular functions are still elusive.

Even as the most extensively studied allergen, the physiological role of Bet v 1 is unknown, although this protein was analysed extensively with biochemical [1,18–22] as well as immunological [1,23–27] methods, and speculations about its physiological role vary widely [28–30]. The crystal and NMR structures of the most abundant Bet v 1 isoform, Bet v 1a (Bet v 1.0101) [21], show a globular protein comprising a seven-stranded anti-parallel β-sheet closed by a 25-residue C-terminal α-helix that is clasped by two short α-helices in a V-shape. The protein contains a glycine-rich loop motif (GXGGXG) that is highly conserved throughout the PR-10 family. All structural elements form a huge hydrophobic pocket [21], a feature that suggested Bet v 1 to function as a carrier or a storage protein. Bet v 1a is able to bind to different ligands *in vitro*, including flavonoids, cytokinins and fatty acids, with micromolar dissociation constants, and the hydrophobic pocket was implied as the binding region [28]. Interestingly, two deoxycholate molecules, aligned in tandem and nearly completely protected from the solvent, were found inside the Bet v 1l hydrophobic pocket [29]. The Bet v 1 homologue PR-10c [31] interacts with cytokinin, flavonoid glycosides, sterols and emodin, and the hydrophobic cavity was again suggested as a binding epitope [32]. Crystal structures of Bet v 1a and Bet v 1j (Bet v 1.0801) [19] in complex with a set of ligands including ANS (1-anilino-8-naphthalene sulfonate), deoxycholate, kinetin and naringenin revealed that these ligands occupy different regions within the hydrophobic pocket and that differences in ligand binding exist between the different isoforms [33].

In spite of all these studies, no physiological ligand of Bet v 1 has been identified as yet. In the present study, we show the isolation of Bet v 1 from mature birch pollen naturally containing Q3OS (quercetin-3-*O*-sophoroside) as an initial hint to the function of this protein and other pollen and food allergens.

EXPERIMENTAL

Isolation of Bet v 1 from birch pollen

The isolation of Bet v 1 from mature birch pollen is on the basis of the observation that the protein could be detected in

Abbreviations: CSP, chemical shift perturbation; DAD, diode array detection; HSQC, heteronuclear single quantum coherence; PR-10, pathogenesis-related proteins 10; Q3OS, quercetin-3-*O*-sophoroside; STD, saturation transfer difference; TIC, total ion chromatogram; UPLC, ultra-performance liquid chromatography; UV/VIS, UV-visible spectroscopy.

[1] To whom correspondence should be addressed (email Olivia.Hartl-Spiegelhauer@uni-bayreuth.de).

© The Authors Journal compilation © 2014 Biochemical Society

the aqueous supernatant of rehydrated pollen [34]. The extraction was conducted as published previously [35] with minor changes. As the basic material, we used 5 g of birch pollen (Allergon) that was incubated in 100 ml of extraction buffer [10 mM potassium phosphate, 1 mM EDTA, 0.1 % ascorbic acid, 4 mM DTT and one Complete™ protease inhibitor cocktail tablet (EDTA-free, Roche), pH 7.0] at 4 °C overnight. The supernatant was precipitated with ammonium sulfate, and the Bet-v-1-containing fractions were pooled. HIC (hydrophobic interaction chromatography) (Octyl Sepharose 4 Fast Flow, 5 ml bed volume, GE Healthcare) was used to further purify and concentrate the samples according to the manufacturer's protocol, and the remaining impurities were removed by gel-filtration chromatography after concentrating the Bet v 1 fractions to a volume of 500 μl with VIVASPIN 20 concentrators (molecular-mass cut-off 3000 Da, Sartorius Stedim Biotech). Subsequently, the protein was loaded on to two sequentially connected Superdex 75 10/300 GL columns (24 ml bed volume each, GE Healthcare), equilibrated with 10 mM potassium phosphate and 300 mM NaCl buffer, pH 7.0, and then the Bet v 1 fractions were pooled and concentrated to a volume of 500 μl. This purification step was then repeated. The columns were calibrated with albumin (67.0 kDa), ovalbumin (43.0 kDa), carbonic anhydrase (29.0 kDa) and ribonuclease A (13.7 kDa). The final protein fractions were freeze-dried and further analysed by MS. All purification steps were followed by UV/VIS (UV–visible spectroscopy) and SDS/PAGE (19 % gel). The most prominent protein bands in the range of 17 kDa were excised and analysed by tryptic digestion followed by LC-MS (Bioanalytics/Center for Molecular Medicine, University of Cologne, Germany) to confirm their identity with Bet v 1.

Pollen extraction for HPLC analysis

Birch pollen was extracted with methanol at room temperature (21 °C) overnight. After centrifugation, the supernatant was concentrated until dry under reduced pressure (40 °C), redissolved in methanol and centrifuged before HPLC analysis.

Preparative RP18–HPLC–UV/ESI–MS^n

Purification of Q3OS was performed using a preparative HPLC–UV/ESI–MS^n system. The Jasco HPLC system consisted of two Jasco PU-2087 Plus pumps connected to a Jasco UV-2075 Plus variable wavelength detector set at 370 nm, an Advantec CHF122SC fraction collector (Tokyo Seisakusho Kaisha) and an Agilent LC/MSD Trap XCT mass spectrometer (Agilent). The column was a Synergi 4u Fusion-RP 80, 25 cm × 21.5 mm (Phenomenex). The HPLC solvents were 0.1 % formic acid in water (A), 0.1 % formic acid in methanol (B) and 0.1 % formic acid in acetonitrile (C). For separation of Q3OS, gradients from 0 % B and 100 % A for 2 min, then to 100 % B in 28 min, 5 min under these conditions, returning to 100 % A and 0 % B at a flow rate of 9.5 ml/min were used. Approximately 2 % were diverted to the mass spectrometer and 9.3 ml fractions were collected. The fraction containing Q3OS was further purified by gradients from 0 % C and 100 % A for 2 min, then to 30 % C and 70 % A in 28 min, followed by 5 min at 100 % C, finally returning to 100 % A. Ionization parameters were as follows: the voltage of the capillary was -4000 V and the end plate was set to -500 V. The temperature of the dry gas (N_2) was 330 °C at a flow of 9 l/min. The full scan mass spectra of the metabolites were measured from *m/z* 50 to 800 until the ICC (ion charge control) target reached 70000 or 200 ms, whichever was reached first. MS^2 was performed using helium as the collision gas, and the collision energy was set at 1.0 V. The target mass for MS^2 spectra was set to *m/z* 625. Mass spectra were acquired in the negative ionization mode. Data analyses were performed using the ChromPass Version 1.9.302.1124 software (Jasco) and the 6300 Series Trap Control Version 6.2 software (Bruker).

UPLC (ultra-performance liquid chromatography)–TOF-MS

High-resolution mass spectra of Q3OS were measured on a Waters Synapt G2 HDMS mass spectrometer (Waters) coupled with an Acquity UPLC core system (Waters) consisting of a binary solvent manager, sample manager and column oven. Aliquots (1 μl) of samples (2 μl) were injected into the UPLC–TOF-MS system equipped with a BEH C_{18} column (2 mm × 150 mm, 1.7 μm, Waters). Operated with a flow rate of 0.3 ml/min at a temperature of 40 °C, the following gradient was used for chromatography: starting with a mixture (35:95, v/v) of acetonitrile (0.1 % HCOOH) and aqueous formic acid (0.1 % HCOOH), the acetonitrile content was increased to 95 % within 3 min and then kept constant for 1 min. Scan time for the MSE method (centroid) was set to 0.1 s. Measurements were performed using negative ESI and the resolution mode consisting of the following ion source parameters: capillary voltage -2.0 kV, sampling cone 20, extraction cone 4.0, source temperature 150 °C, desolvation temperature 450 °C, cone gas 30 l/h and desolvation gas 850 l/h. Data processing was performed by using MassLynx 4.1 SCN 779 (Waters) and the elemental composition tool for determining the exact mass. All data were lock mass corrected on the pentapeptide leucine enkephalin (YGGFL, *m/z* 554.2615, $[M-H]^-$) in a solution (2 ng/μl) of acetonitrile/0.1 % formic acid (1:1, v/v). Scan time for the lock mass was set to 0.3 s, an interval of 15 and three scans to average with a mass window of $\pm$0.3 Da. Calibration of the Synapt G2 apparatus in the range *m/z* 50–600 was performed using a solution of sodium formate (5 mmol/l) in 2-propanol/water (9:1, v/v).

NMR spectroscopy of Q3OS

^{1}H-NMR and ^{13}C spectroscopy of Q3OS was performed on an Avance III 500 MHz spectrometer with a TCI Cryo Probe (Bruker). Chemical shifts were referenced to TMS (tetramethylsilane). Data processing was performed with Topspin version 1.3 (Bruker) and MestReNova version 5.2.3 software (Mestrelab Research).

Expression and purification of Bet v 1a

The Bet v 1a gene was cloned into the bacterial expression vector pET-11a (Novagen) with the restriction enzymes NdeI and BpU 1102I (Fermentas). The gene was expressed in *Escherichia coli* strain BL21(DE3) cells growing at 37 °C in 1 litre of LB medium, supplemented with 100 μg/ml ampicillin to a D_{600} value of 0.6. A final concentration of 1 mM IPTG was added to the medium to induce the protein expression. To obtain ^{15}N-labelled Bet v 1a, overexpressing *E. coli* were grown on M9 minimal medium with ^{15}N-enriched $(^{15}NH4)_2SO_4$. The cells were harvested 4 h after induction by centrifugation (5500 ***g***, 10 min, 4 °C), and the cell pellets were stored at -20 °C.

For protein purification the frozen cells were resuspended in 20 mM Tris buffer, pH 8.0, containing one Complete™ protease inhibitor cocktail tablet (EDTA-free, Roche), lysozyme and DNase. The cells were stirred on ice for 30 min followed by lysis using a microfluidizer. The lysate was centrifuged at 19000 ***g*** for 30 min at 4 °C and PEI (polyethylenimine) was added to the supernatant to a final concentration of 0.35 % to precipitate nucleic acids. The solution was incubated for 15 min at room

© The Authors Journal compilation © 2014 Biochemical Society

temperature and the emerging precipitate was removed by centrifugation (19000 ***g***, 30 min, 4 °C). The clarified protein solution was loaded on to a 10-ml Q XL Sepharose column (HiTrap Q XL, GE Healthcare) and was eluted using a stepwise gradient including 10, 15, 20 and 100 % (v/v) elution buffer (20 mM Tris buffer, pH 8.0, and 300 mM NaCl). Fractions were then analysed by SDS/PAGE (19 % gel). Bet v 1-containing fractions were pooled and dialysed for at least 4 h at 4 °C against Millipore water and finally the protein was freeze-dried and stored at 4 °C.

Cell culture (1 litre) from LB and M9 minimal medium yielded approximately 32 and 18 mg of Bet v 1 respectively. Protein concentrations were determined by the DC protein assay (Bio-Rad Laboratories) and UV/VIS using the molar extinction coefficient $\varepsilon_{280} = 10430\ M^{-1} \cdot cm^{-1}$.

Reconstitution of Bet v 1a–Q3OS

For reconstitution we used final concentrations of 500 μM Bet v 1a and excess amounts of Q3OS in 10 mM sodium phosphate buffer, pH 7.0, in a total volume of 500 μl. The sample was loaded on to two sequentially connected Superdex 75 10/300 GL columns (24 ml bed volume each, GE Healthcare) equilibrated with sample buffer containing 300 mM NaCl. The isocratic protein elution was carried out at a flow rate of 0.4 ml/min. In addition, a sample of Q3OS with identical concentrations and volumes was loaded separately for comparison.

UV/VIS

Quercetin (Sigma–Aldrich) and Q3OS were dissolved in 50 mM sodium phosphate, 50 mM NaCl and 10 % (v/v) DMSO buffer, pH 7.0, to a final concentration of 20 μM. The solutions (500 μl) were used for the titration with Bet v 1a in a 1 cm quartz cuvette (Hellma Analytics) at 25 °C. The titrations were performed by adding small amounts of a 2 mM Bet v 1a stock solution prepared in the same buffer. Absorption spectra from 200 to 800 nm were recorded using an Agilent 8453 UV-visible spectrophotometer. Changes of absorption at 320 nm for quercetin and 358 nm for Q3OS were plotted against Bet v 1a concentration. Before curve fitting, absorbance data were corrected for dilution. If possible, the equilibrium dissociation constant (K_d) was determined by non-linear regression analysis of the data with GraFit-5 (version 5.0, Erithacus Software) using eqn (1):

$$\Delta A = \frac{\Delta A_{max}}{2Q}\left\{(B + Q + K_d) - \left[(B + Q + K_d)^2 - (4BQ)^{0.5}\right]\right\} \quad (1)$$

where ΔA_{max} is the maximum change in absorbance at specific wavelengths; B is Bet v 1a concentration; and Q is total flavonoid concentration.

In all titration experiments a suitable amount of DMSO was present to avoid solubility problems and therefore to disable unwanted side effects of the flavonoids. With HSQC (heteronuclear single quantum coherence) NMR measurements of Bet v 1a, we could exclude aggregation or partial unfolding of the protein in the presence of increasing DMSO concentrations (see Supplementary Figure S6). Additionally, titration experiments at different DMSO concentrations indicate that there is only a very small increase in the K_d value at rising DMSO concentrations.

Fluorescence spectroscopy

For fluorescence equilibrium titrations the intrinsic fluorescence of protein-bound Q3OS was used. The measurements were carried out with a Horiba Fluoromax fluorimeter at 25 °C in fluorescence buffer [50 mM sodium phosphate buffer, pH 7.0, containing 50 mM NaCl and 10 % (v/v) DMSO] in a total volume of 1 ml using a 10 mm × 4 mm quartz cuvette (Hellma Analytics). Q3OS was provided at a concentration of 500 nM and Bet v 1a was added in 10 μl steps from a 50 μM stock solution. The excitation wavelength was 340 nm, and emission spectra were measured from 410 to 430 nm. Slit widths were set at 6 nm for excitation and emission. Data were analysed by plotting the relative change of fluorescence intensity at 416 nm against increasing concentrations of Bet v 1a corrected for dilution. The equilibrium dissociation constant (K_d) was determined from data fitted to eqn (2) by non-linear regression using GraFit-5 software (version 5.0, Erithacus Software):

$$\Delta F_{norm} = \frac{\Delta F_{max} \cdot \left[(Q + B + K_d) - \sqrt{(Q + B + K_d)^2 - (4QB)}\right]}{2Q} \quad (2)$$

where ΔF_{norm} is the normalized change in fluorescence; B is Bet v 1a concentration; Q is total concentration flavonoid; and ΔF_{max} is maximum fluorescence change.

Protein NMR spectroscopy

All NMR experiments were performed at 298 K in 50 mM sodium phosphate buffer, 50 mM NaCl, pH 7.0, and 10 % ^2H_2O with ^{15}N uniformly labelled Bet v 1a using Bruker Avance 700 MHz and Avance 800 MHz spectrometers with cryogenically cooled triple-resonance probes equipped with pulsed field-gradient capabilities. NMR data were processed using in-house software and visualized with NMRViewJ [36]. The sequence-specific assignments of the amide resonances of Bet v 1a are reported elsewhere [22].

For the different titration experiments quercetin and rutin stock solutions were prepared in deuterated DMSO and Q3OS and sophorose stock solutions were prepared in 50 mM sodium phosphate and 50 mM NaCl buffer, pH 7.0, containing 100 μM Bet v 1a. Rutin and Q3OS were added in a single step, whereas quercetin and sophorose were added stepwise to a final excess of 1:15 to the protein sample; final DMSO concentrations did not exceed 13.5 % (v/v). CSPs (chemical shift perturbations) caused by increasing DMSO concentrations within the measurements of quercetin and rutin were identified by titrating DMSO in comparable steps. CSPs were calculated using eqn (3):

$$\Delta\delta_{norm} = \sqrt{(\Delta\delta_{HN})^2 + (0.1 \cdot \Delta\delta_N)^2} \quad (3)$$

where $\Delta\delta_{HN}$ and $\Delta\delta_N$ are chemical shift differences in amide proton and nitrogen resonances respectively in p.p.m. The K_d value for quercetin binding was determined with NMRViewJ [36]. CSPs from amino acid residues that were unaffected by increasing DMSO concentrations were fit to a quadratic binding curve with default setting, and an average K_d (app) was calculated.

For chemical shift mapping of quercetin and Q3OS binding, different experimental setups were used. Quercetin was added to a 15-fold excess to 100 μM Bet v 1a solution containing 10 % (v/v) DMSO to ensure a constant DMSO concentration. The CSPs were mapped on to the Bet v 1a structure (PDB code 1BV1). Titration experiments with Q3OS were performed by stepwise addition of Bet v 1a to a 680 μM sample of Q3OS to Q3OS/Bet v 1a ratios of 15:1 to 2.4:1. Only amino acids in which signals disappear following Q3OS binding were labelled in the Bet v 1a structure.

For the displacement experiment, 100 μM Bet v 1a and 25 μM quercetin were used in the same buffer without DMSO. Q3OS was added from a stock solution to a final excess of 1:10 over Bet v 1a.

© The Authors Journal compilation © 2014 Biochemical Society

STD (saturation transfer difference) NMR spectroscopy

All experiments were performed on a Bruker Avance 600 MHz spectrometer equipped with a standard triple resonance probe. NMR samples were prepared in 550 μl of 99.85 % ^2H_2O buffer containing 50 mM sodium phosphate and 50 mM NaCl, pH 7.0, with 2 mM of Q3OS (and 4 % d_6-DMSO) or sophorose respectively. Bet v 1a was added from a stock of 3.42 mM to a final concentration of 225 μM.

For the STD NMR experiments, a saturation period with on/off resonance continuous wave saturation of 4 s was applied. The on-resonance frequency was set to 0.7 p.p.m. and the off-resonance frequency was set to 20 p.p.m. Protein signals were suppressed by using a spinlock pulse of 50 ms.

Docking simulation

We used AutoDockVina [37] to dock Q3OS into the hydrophobic pocket of Bet v 1a. The allergen listed under PDB code 4A87 served as a template for Bet v 1a. The PDB file for Q3OS was created with ProDrg [38]. Furthermore, input files for Bet v 1a and Q3OS were generated with AutoDockTools [39]. The grid box ($20\,\text{Å} \times 24\,\text{Å} \times 28\,\text{Å}$ or $13\,440\,\text{Å}^3$) (1 Å = 0.1 nm) was centred over the hydrophobic pocket of Bet v 1a and AutoDockVina was run with default settings. Affinity scores were given by AutoDockVina as binding energies (ΔG), which were subsequently used to calculate an equilibrium dissociation constant (K_d) by eqn (4) with $R = 0.001968\,\text{kcal} \cdot \text{mol}^{-1} \cdot \text{K}^{-1}$ and $T = 298.15$ K:

$$K_d = e^{\frac{-\Delta G}{R \cdot T}} \quad (4)$$

The docking simulations resulted in nine different possible orientations of Q3OS in the Bet v 1a pocket. Seven models show similar binding for the quercetin moiety, whereas the binding situation for the sugar moiety is less defined. The model in best agreement with our experimental NMR data was chosen to illustrate Q3OS binding to Bet v 1.

RESULTS

Isolation of Bet v 1 from mature birch pollen

Extraction of Bet v 1 from mature birch pollen [35] yielded SEC (size exclusion chromatography) fractions containing Bet v 1 that were brightly yellow coloured, and the colour persisted during protein concentration (Supplementary Figure S1 at http://www.biochemj.org/bj/457/bj4570379add.htm). UV/VIS absorption spectra of these fractions had a maximum at 350 nm, which was subsequently used to detect the protein-bound ligand during LC. The protein (280 nm) and the coloured ligand (350 nm) both eluted from the SEC column at a volume of 23 ml as almost pure compounds (Figure 1A). The protein fractions exhibit a minimum of three intense and closely spaced protein bands in the SDS/PAGE (Figure 1B), corresponding to molecular masses of approximately 17 kDa. UPLC–TOF-MS identified Bet v 1a (Bet v 1.0101), Bet v 1d (Bet v 1.0401), Bet v 1f (Bet v 1.0601), Bet v 1g (Bet v 1.0701) and Bet v 1m (Bet v 1.1401) as components of the protein fractions. The mixture of isoforms will be termed Bet v 1 for simplicity in the present paper.

Identification of the bound ligand

The biochemically purified Bet v 1 protein was freeze-dried. The yellowish residue was extracted with water/methanol (1:1), centrifuged and the supernatant analysed by LC-DAD (diode array detection)-MS. The UV trace (200–600 nm) and the TIC (total ion chromatogram) showed only one single compound (Figure 2, lower two traces), exhibiting UV maxima at 252 and 358 nm as well as pseudomolecular ions of *m/z* 625 $[M-H]^-$ and 649 $[M+Na]^+$ in the negative and positive ion mode respectively (Supplementary Figures S2A, S2B and S2D at http://www.biochemj.org/bj/457/bj4570379add.htm). The fragmentation patterns indicated the presence of up to two glucose residues in the molecule (Supplementary Figures S2C and S2E). The molecular mass (626 g/mol) of the metabolite was confirmed by LC-TOF analysis and provided a putative sum formula of $C_{27}H_{29}O_{17}$ for the isolated product (Supplementary Figure S3 at http://www.biochemj.org/bj/457/bj4570379add.htm), suggesting the presence of a quercetin dihexoside. Since the amount of the material isolated from the Bet v 1 protein was too low for NMR analysis we purified a larger quantity from birch pollen by preparative LC. The comparison of the ^{1}H- and ^{13}C-NMR spectra (Supplementary Figures S4 and S5 at http://www.biochemj.org/bj/457/bj4570379add.htm) of the isolated metabolite with those of different flavonol diglycosides yielded Q3OS (Figure 1C, and Supplementary Table S1 at http://www.biochemj.org/bj/457/bj4570379add.htm) as the structure for the natural ligand of Bet v 1. Although the birch pollen extract contained numerous phenolic glycosides (Figure 2, upper two traces) only Q3OS was co-purified with the Bet v 1 protein (Figure 2, lower two traces).

Reconstitution of Bet v 1a–Q3OS

We reconstituted Bet v 1–Q3OS by adding the ligand to recombinantly produced protein. SEC analysis yielded an elution diagram basically identical to that of the natural complex (Figures 1D and 1E). A minor amount of ligand eluted at a volume of 35 ml as identified by SEC analysis of Q3OS alone (Figure 1D, grey line).

UV/VIS/fluorescence titrations

To determine equilibrium dissociation constants (K_d), we followed the titration of Q3OS and quercetin with Bet v 1a by UV/VIS (Figures 3A–3D). The spectra of the titration of quercetin with Bet v 1a show isosbestic points indicating a two-state binding process for the flavonoid (Figure 3A) with $K_d = 9.2 \pm 0.6$ μM (Figure 3B).

For the Q3OS titration with Bet v 1 only small changes in the absorbance spectrum could be observed (Figure 3C), and we could not obtain analysable data, although isosbestic points indicated complex formation (Figure 3D).

We performed a fluorescence titration in tandem with the UV/VIS titrations to determine the K_d value for Q3OS binding to Bet v 1 (Figure 3E). In contrast with the UV/VIS experiment, the fluorescence data were analysable and yielded $K_d = 566 \pm 85$ nM (Figure 3F).

NMR spectroscopy

To study the binding behaviour of quercetin, Q3OS, rutin and sophorose to Bet v 1 and to identify ligand binding sites on Bet v 1 we employed CSP measurements with ^{1}H-^{15}N HSQC NMR spectroscopy. Addition of the compounds to ^{15}N-labelled Bet v 1a in protein/ligand ratios of 1:0.1 to 1:15 led to clearly observable compound-specific changes in the ^{1}H-^{15}N HSQC spectra (Figure 4). Since DMSO is indispensable in the measurement to ensure the solubility of quercetin we had to take into account the effect of increasing DMSO concentrations on the CSPs (Supplementary Figure S6 at http://www.biochemj.org/bj/457/bj4570379add.htm).

© The Authors Journal compilation © 2014 Biochemical Society

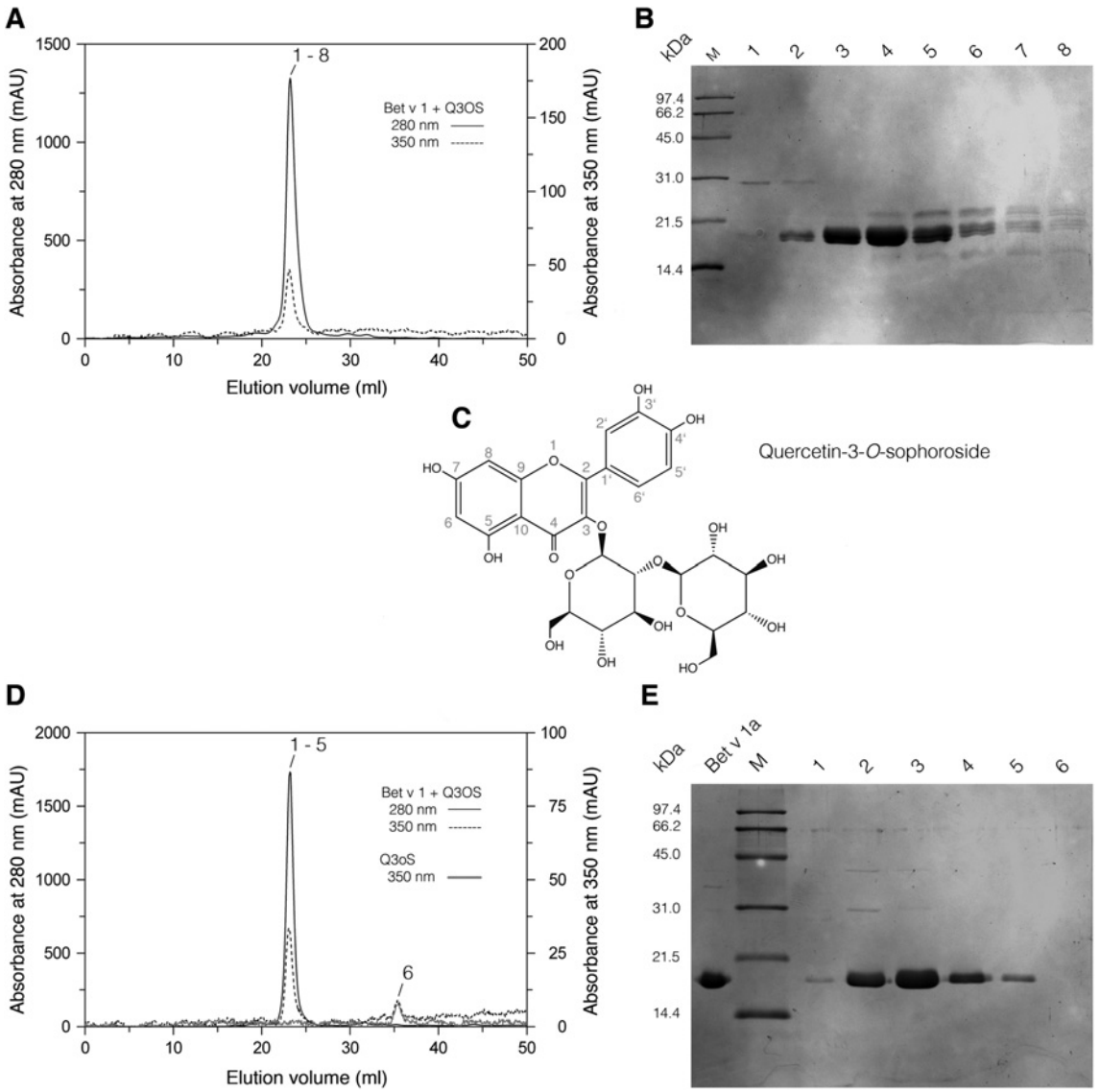


Figure 1 Identification of Q3OS as a ligand of Bet v 1

(**A**) SEC of Bet v 1 isolated from mature birch pollen with two sequentially connected Superdex S75 10/300 GL columns performed in 10 mM phosphate buffer, pH 7.0, and 300 mM NaCl. The traces correspond to absorbance at 280 nm (continuous line) and 350 nm (broken line). (**B**) Corresponding analysis of the SEC fractions by SDS/PAGE (19 % gel). M, molecular-mass standard (SDS/PAGE Molecular Weight Standards, Low Range, Bio-Rad Laboratories). Lanes 1–8, proteins eluted within the 20 and 25 ml elution volumes. (**C**) Structure of the identified ligand Q3OS. (**D**) SEC analysis of the reconstitution of recombinant Bet v 1a–Q3OS. The continuous and broken black traces correspond to the run of Bet v 1–Q3OS with absorbance measured at 280 and 350 nm respectively. The grey line corresponds to a run of Q3OS alone with absorbance measured at 350 nm. (**E**) Analysis of the SEC fractions of Bet v 1–Q3OS by SDS/PAGE (19 % gel). Bet v 1a, recombinantly purified protein. M, molecular-mass standard (SDS/PAGE Molecular Weight Standard, Low Range, Bio-Rad Laboratories). Lanes 1–6, Bet v 1a–Q3OS eluted within the 20 and 25 ml elution volumes.

For quercetin, gradual CSPs in the ^{1}H-^{15}N HSQC spectra could be observed which are characteristic for complex formation in the fast-exchange regime of the NMR time scale (Figure 4A, and Supplementary Figure S7 at http://www.biochemj.org/bj/457/bj4570379add.htm). The K_d value was determined from CSPs of amino acids that are not affected by DMSO as 33 ± 2 μM, in agreement with the UV/VIS measurements. Titration of Bet v 1a with Q3OS led to ^{1}H-^{15}N HSQC spectra with peaks of several residues disappearing completely during titration, which is characteristic for intermediate exchange rates (Figure 4B, and Supplementary Figure S8 at http://www.biochemj.org/bj/457/bj4570379add.htm). This does not allow a proper line shape analysis for determination of the dissociation constant. However, this observation is in agreement with the K_d value gained from the fluorescence titration.

Very small CSPs even at higher rutin concentrations indicated very weak rutin binding to Bet v 1a (Figure 4C, and Supplementary Figure S9 at http://www.biochemj.org/bj/457/bj4570379add.htm). No CSPs and thus no conclusive evidence of Bet v 1a interaction could be observed during sophorose titration (Figure 4D and Supplementary Figure S10 at http://www.biochemj.org/bj/457/bj4570379add.htm). In addition, we performed STD NMR experiments with Bet v 1a and sophorose, a technique used to investigate very weak interactions between proteins and ligands. Still, we were not able to detect any interactions between the two molecules. Remarkably, quercetin can be partially displaced from Bet v 1a by addition of Q3OS in competition ^{1}H-^{15}N HSQC experiments with ^{15}N-labelled Bet v 1a, quercetin and added Q3OS (Supplementary Figure S11 at http://www.biochemj.org/bj/457/bj4570379add.htm).

© The Authors Journal compilation © 2014 Biochemical Society

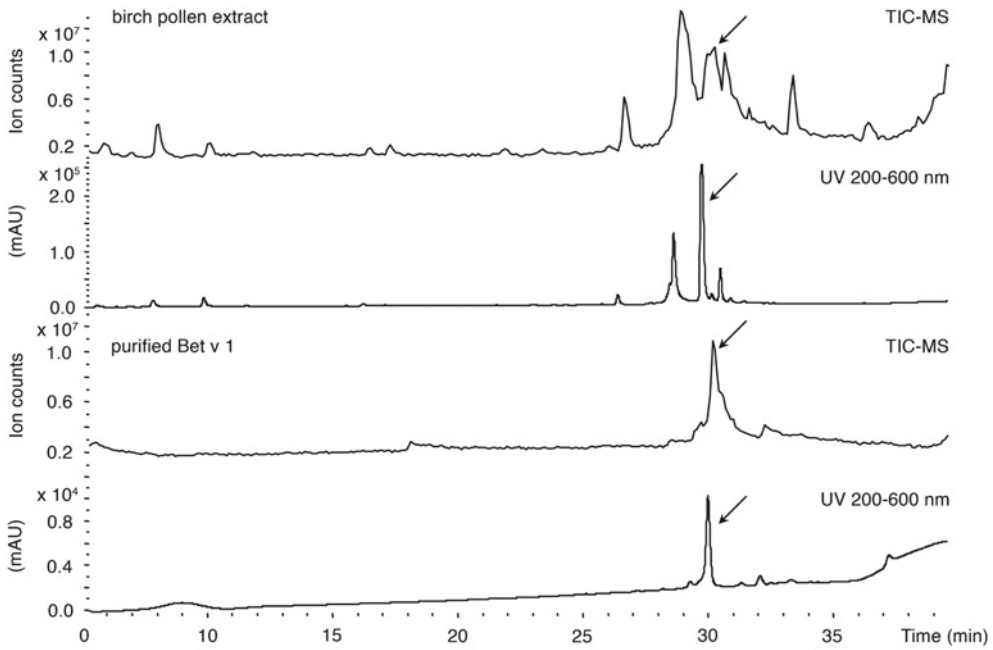


Figure 2 Co-purification of Q3OS with the Bet v 1 protein

LC-DAD-MS analysis of a birch pollen extract and the purified Bet v 1 protein obtained by ammonium sulfate precipitation followed by hydrophobic interaction and SEC. The TIC acquired in the negative mode (TIC-MS) and the UV trace (200–600 nm) show different metabolites of the birch pollen extract (upper two traces), whereas Q3OS (arrow) is highly enriched in the purified Bet v 1 protein (lower two traces).

In different ^{1}H-^{15}N HSQC experiments, we analysed the interaction surfaces of quercetin and Q3OS with Bet v 1. Quercetin was added to ^{15}N-labelled Bet v 1a containing 10 % (v/v) DMSO to neutralize the effects of DMSO addition on the CSPs (Supplementary Figure S12 at http://www.biochemj.org/bj/457/bj4570379add.htm). Thus we could safely map residues showing CSPs larger than 0.04 p.p.m. following addition of quercetin on to the structure of Bet v 1a (Figure 5A). Most residues that showed significant CSPs (e.g. Thr^{10}, Lys^{115} and Lys^{137}–Leu^{143}) were found in the region around the C-terminal helix. To study Q3OS binding, the protein was added stepwise to a concentrated sample of Q3OS (Supplementary Figure S13 at http://www.biochemj.org/bj/457/bj4570379add.htm). Amino acids with disappearing signals were mapped on the Bet v 1 structure (Figure 5B). Surprisingly, most of these amino acids were also located around the C-terminal helix, indicating that the glycosylation does not severely change the binding properties of the quercetin moiety. A structural model confirmed the binding situation of the Bet v 1a–Q3OS complex and provided an estimated K_d value of 1.7 μM (Figure 5D). Although the docking simulation demonstrates that the Bet v 1a pocket is, in general, large enough to easily allow Q3OS binding, the exact binding geometry of the disaccharide moiety still remains elusive.

DISCUSSION

The physiological role of PR-10 and, therefore allergenic, proteins in this family is poorly understood. However, the biological function is important even for the understanding of allergenicity of proteins, as it is still unknown whether structural features as such are responsible for the immune response or whether additional functional properties are also important factors [40].

Identification of the natural ligand of Bet v 1

All Bet-v-1-containing fractions that were obtained during the purification process displayed a yellow colour and even during SEC the colour could be used as an indicator for spotting the samples with the allergen (Figure 1A). LC-DAD-MS analyses confirmed the co-purification of a single UV active compound, which was also detected in the initial birch pollen extract among numerous other metabolites (Figure 2). The natural ligand was unambiguously identified as Q3OS according to its LC-DAD-MS and NMR data. Sophorose [glucosyl(1-2)-β-glucose] was first isolated from *Sophora japonica* in which it occurs as kaempferol-3-*O*-sophoroside. Subsequent studies showed that the sugar is attached to anthocyanins and flavones isolated from many plant sources [41], and pollen seem to be particularly rich in 3-*O*-sophorosides of kaempferol and quercetin [42,43]. Although from prior binding studies, it was expected that flavonols may be natural ligands of Bet v 1, it was surprising to find a glycosylated compound as natural Bet v 1 ligand.

Binding of quercetin and Q3OS

To investigate Q3OS–Bet v 1 interaction we used the recombinantly purified isoform Bet v 1a. Q3OS was not only identified as a ligand of Bet v 1 purified from mature birch pollen, but also bound strongly to recombinant Bet v 1a in a reconstitution experiment (see Figure 1). The identical elution profiles of the Bet v 1a–ligand complexes confirm that Q3OS is indeed a physiological binding partner of Bet v 1.

We performed various NMR experiments with Q3OS and its quercetin and sugar moiety in order to locate the binding site of Q3OS on Bet v 1. In an initial experiment with quercetin, significant CSPs in the protein could be determined and mapped on to the Bet v 1a structure (Figure 5A). Most of the affected residues lie in a region around the centre of the long C-terminal

© The Authors Journal compilation © 2014 Biochemical Society

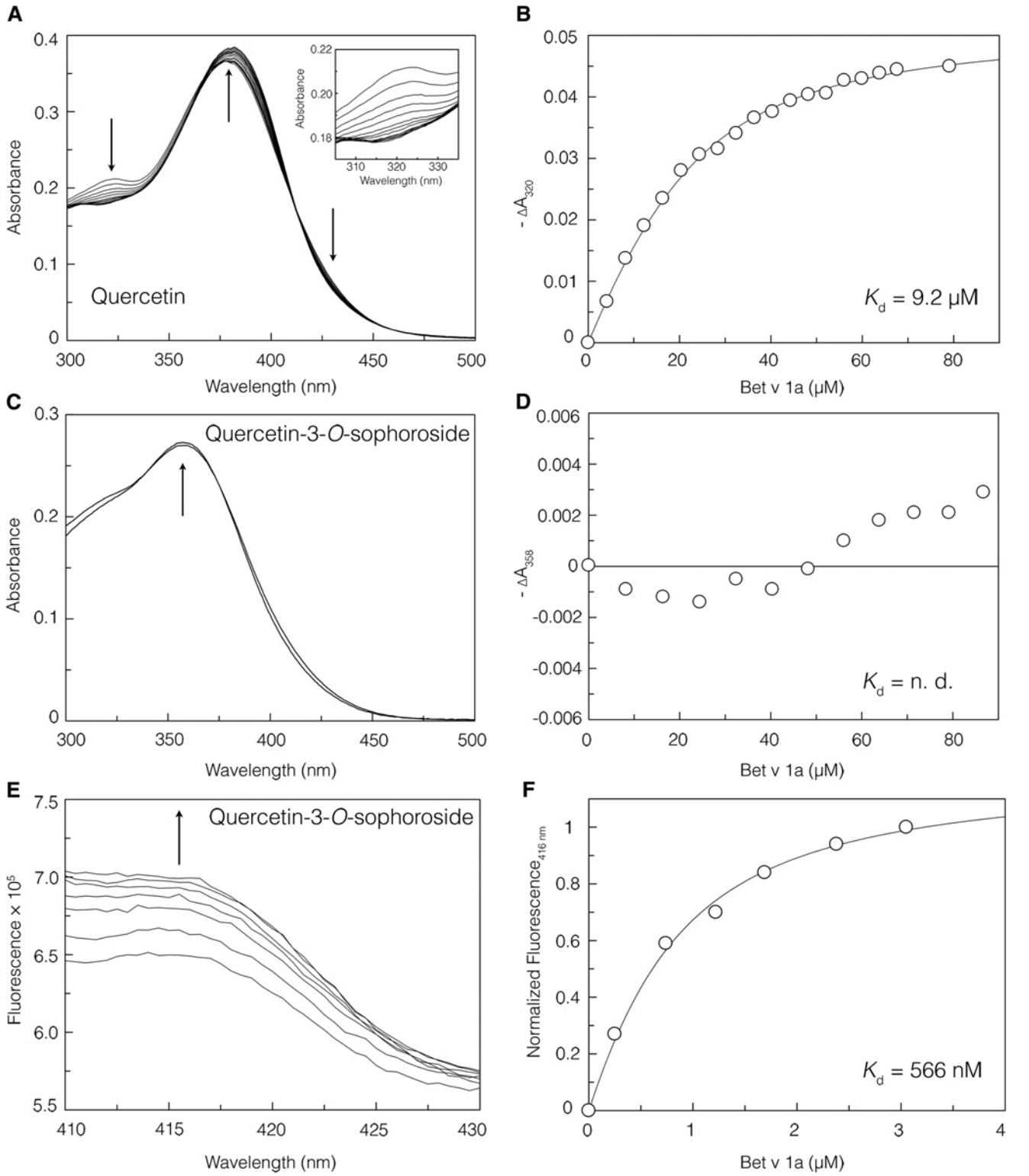


Figure 3 Binding interactions of Bet v 1 with quercetin and Q3OS

Measurements were carried out in 50 mM sodium phosphate buffer, pH 7.0, containing 50 mM NaCl and 10 % (v/v) DMSO at 25 °C. (**A**) UV/VIS spectra of the equilibrium titration of 20 μM quercetin with increasing concentrations of Bet v 1a. (**B**) Absorbance changes at 320 nm against Bet v 1a concentrations for the data as shown in (**A**). The curve shows the best fit to eqn (1). (**C**) Initial and final spectrum of the UV/VIS equilibrium titration of 20 μM Q3OS with increasing concentrations of Bet v 1a. (**D**) Absorbance changes at 358 nm against Bet v 1a concentrations for the data shown in (**C**). (**E**) Fluorescence spectra of the equilibrium titration of 500 nM Q3OS with Bet v 1a. (**F**) Fluorescence changes at 416 nm against Bet v 1a concentrations for the data shown in (**E**). The curve shows the best fit to eqn (2).

© The Authors Journal compilation © 2014 Biochemical Society

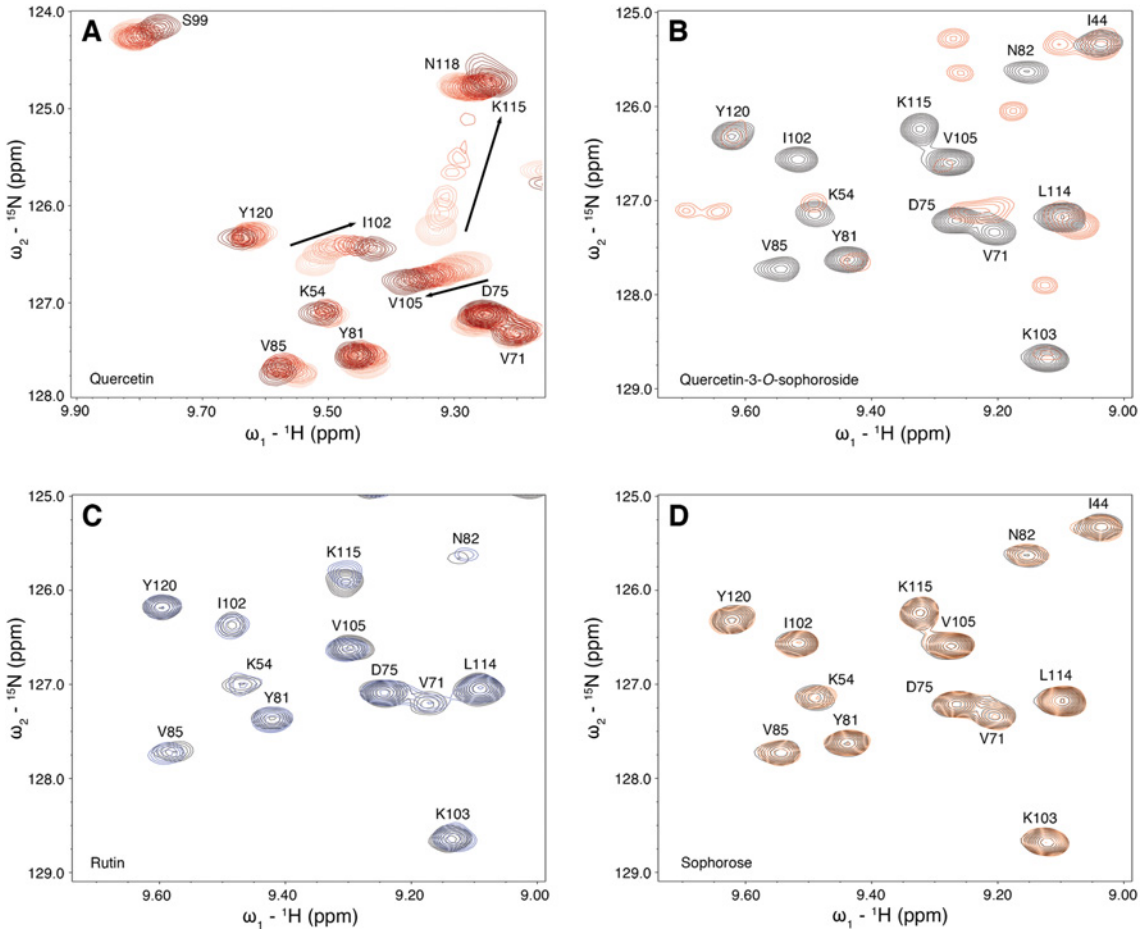


Figure 4 NMR equilibrium titration experiments of Bet v 1a and different compounds

All experiments were performed with 100 μM ^{15}N-uniformly labelled Bet v 1a at 298 K in 50 mM sodium phosphate buffer, pH 7.0, 50 mM NaCl and 10 % $^{2}H_2O$ with Bruker Avance 700 MHz and Avance 800 MHz spectrometers. (**A**) Overlay of ten ^{1}H-^{15}N HSQC spectra of Bet v 1a in the presence of increasing quercetin (DMSO) concentrations, from light to dark red. Quercetin was added from a stock solution prepared in deuterated DMSO to a final excess of 1:15 over Bet v 1a and a final DMSO concentration of 13.5 % (v/v). ^{1}H-^{15}N chemical shift changes (indicated with arrows) of residues Ile^{102}, Val^{105} and Lys^{115} indicate complex formation in the fast-exchange regime. (**B**) Overlay of two ^{1}H-^{15}N HSQC spectra of Bet v 1a in the absence (black) and presence of a 15-fold excess of Q3OS (red). Several ^{1}H-^{15}N resonances (Asn^{82}, Val^{85}, Ile^{102} and Lys^{115}) disappear completely upon addition of Q3OS. Consequently, appearing resonances cannot be identified. (**C**) Overlay of two ^{1}H-^{15}N HSQC spectra of Bet v 1a in the absence (black) and presence (blue) of a 15-fold excess of rutin. In the region shown only residues Asn^{82}, Val^{85} and Lys^{115} show marginal shift changes following addition of rutin. (**D**) Overlay of two ^{1}H-^{15}N HSQC spectra of Bet v 1a in the absence (black) and presence (orange) of a 15-fold excess of sophorose. The addition of sophorose did not result in chemical shift changes of Bet v 1a resonances.

α-helix, in agreement with a recently published structure of a Bet v 1a–naringenin complex [33] (Figure 5C). Naringenin, which lacks the 3′-OH and the 3-OH groups of quercetin (Figure 4), is co-ordinated by hydrogen bonding and hydrophobic interactions between the C-terminal α-helix and the N-terminal β-strand. Contrary to expectations that two or more copies of a small molecule would occupy the large cavity in Bet v 1 [29], a single naringenin molecule is bound and fills only a small fraction of the hydrophobic pocket. Assuming that quercetin is bound in an orientation identical with that of naringenin, the quercetin 3-OH group would point towards the pocket interior which still would provide enough space to accommodate the sophorose residue of Q3OS. As we were not able to assign all residues of Bet v 1 in the presence of Q3OS, we decided to simply use signals with intense signal broadening (‘disappearing’ signals) for chemical shift mapping (Figure 5B). Interestingly, the result is very similar to that for the quercetin titration. This led us to propose that the disappearing signals arise from the quercetin moiety of Q3OS that is bound in the same region as quercetin alone. Hence these data support the notion that quercetin both in its free and glycosylated form binds in naringenin-like fashion.

Additional information on the complex geometry was gained from fluorescence titration and NMR measurements with Q3OS. Not unexpectedly, Q3OS in solution exhibits only marginal fluorescence, as flavonols (like quercetin or Q3OS) containing a 5-OH group (see Figure 1) are generally non-fluorescent due to an intramolecular hydrogen bond between the carbonyl oxygen (position C4) and the 5-OH group that facilitates non-radiative de-excitation [44]. The appearance of a fluorescence signal of Q3OS following Bet v 1a binding (Figure 3E) may indicate that this intramolecular hydrogen bond is distorted and that either the carbonyl oxygen or the 5-OH group or both are somehow involved in the binding process.

The Bet v 1a–naringenin complex structure and our NMR data support this idea. On titration of quercetin to Bet v 1a, several residues (e.g. Phe^{30}, Tyr^{83}, Ile^{102}, Ser^{136} or Glu^{141}) show strong CSPs in the HSQC spectra. These residues are identical with those that are involved in direct hydrogen bonds and hydrophobic contacts with naringenin, except for residue Asn^{118}. In the Bet

© The Authors Journal compilation © 2014 Biochemical Society

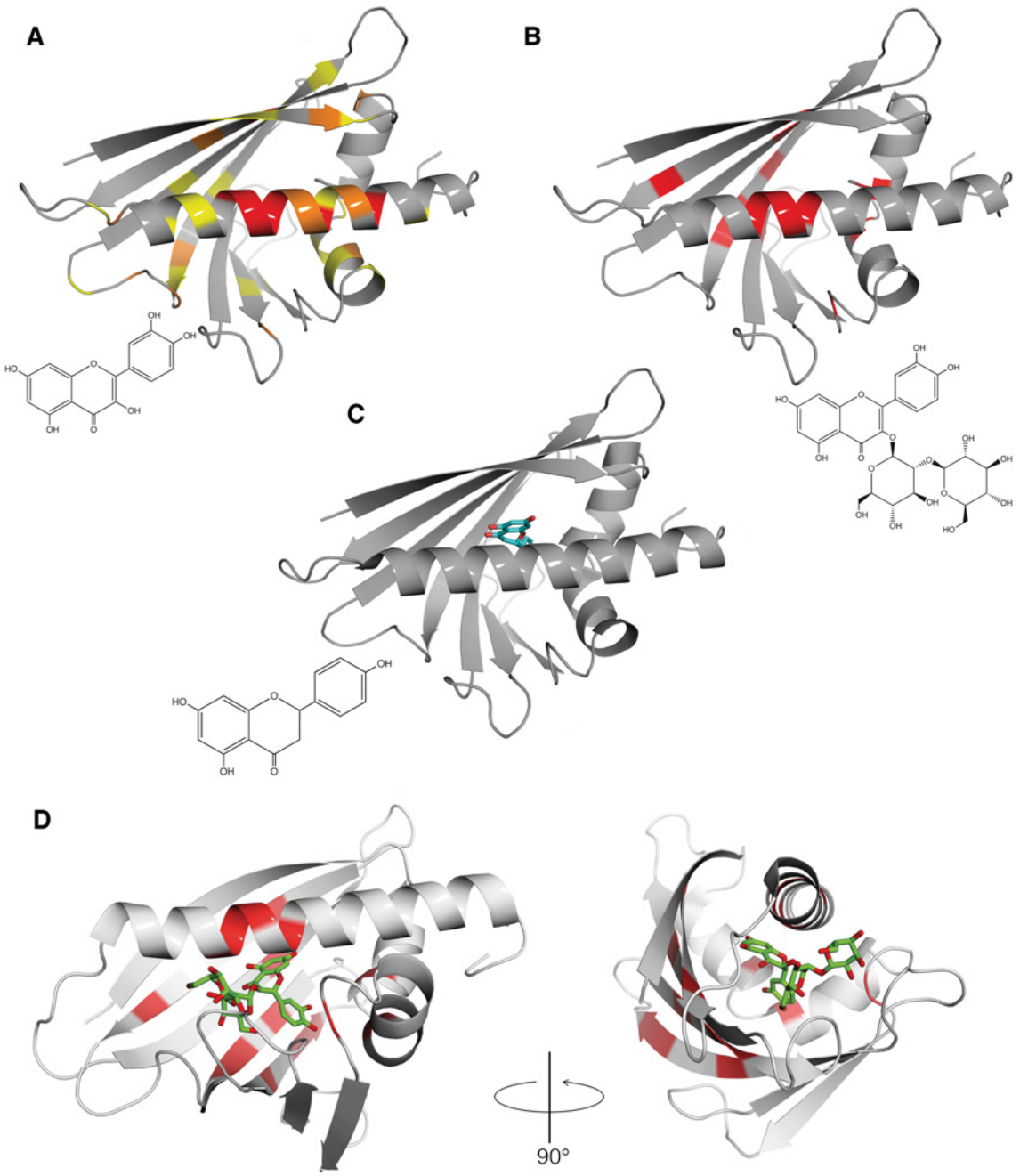


Figure 5 Comparison of the solution structure models of Bet v 1–quercetin, Bet v 1–Q3OS and the crystal structure of the Bet v 1a–naringenin

(**A**) Chemical shift changes ($\Delta\delta$) upon quercetin binding mapped on a cartoon representation of Bet v 1a (PDB code 1BV1; grey); 0.04 p.p.m.$\leqslant\Delta\delta\leqslant$0.08 p.p.m. shown as yellow; 0.08 p.p.m.$<\Delta\delta\leqslant$0.12 p.p.m. shown as orange; and 0.12 p.p.m.$<\Delta\delta$ shown as red. (**B**) as (**A**), with Q3OS. Amino acids whose signals disappear during titration, red. (**C**) Cartoon representation of the crystal structure of Bet v 1a–naringenin (PDB code 4A87). Grey, Bet v 1a; blue sticks, naringenin; red, oxygen. (**D**) Bet v 1a–Q3OS model based on AutoDockVina (based on PDB code 4A87). Grey, Bet v 1a; spectral changes upon Q3OS coded as in (**B**). Green sticks, Q3OS; red, oxygen.

v 1a–naringenin complex the carbonyl oxygen of Asn[118] forms a sodium bridge with the carbonyl oxygen and the 5-OH group of naringenin [33]. This salt bridge may explain the fact that Asn[118] does not show CSPs in our HSQC measurements following quercetin binding, but nevertheless is involved in quercetin binding according to the fluorescence data.

These data strongly support the idea that quercetin, the quercetin moiety of Q3OS, and naringenin bind to the same Bet v 1 region near the C-terminal helix and are oriented similarly. Although the sophorose moiety of Q3OS could not be located experimentally, docking simulations (Figure 5D) were in agreement with the experimental results.

Specificity of Q3OS binding

Next, we asked whether the binding of Q3OS to Bet v 1a is specific. We thus tested the binding characteristics of an additional set of compounds. Rutin was used as an alternative glycosylated

© The Authors Journal compilation © 2014 Biochemical Society

flavonoid as it was shown to interact with the Bet v 1 homologue birch PR-10c [32]. Rutin is a naturally occurring compound composed of the flavonol quercetin and the disaccharide rutinose [α-L-rhamnopyranosyl-(1→6)-β-D-glucopyranose], and it can be found in more than 70 plant species [45]. The difference between Q3OS and rutin is the composition and therefore the geometry of the disaccharide. Our data show only weak interaction between rutin and Bet v 1a (Figure 4C), thus we conclude that the nature of the glycosylation plays an important role and that the Bet v 1 interaction is very specific for Q3OS.

Therefore we studied sophorose binding to the protein. Interestingly, even with a 10- or 15-fold excess of the disaccharide we were not able to detect STD signals or CSPs (Figure 4D) respectively, indicating no or very weak binding. Low affinities for proteins and carbohydrates is a well-reported phenomenon resulting from a balance of a favourable negative enthalpy difference caused by hydrogen bonding, van der Waals or hydrophobic interactions, and a counteracting entropy term caused, e.g. by the restricted carbohydrate geometry or solvation effects [46–50]. This enthalpy–entropy compensation is a general characteristic of weak intermolecular interactions [51]. The different dissociation constants for quercetin (9.2–33 μM), sophorose (no binding) and Q3OS (566 nM) show that the disaccharide in Q3OS causes an up to 60-fold higher affinity of the flavonol, although the carbohydrate alone shows no or only weak binding. Thus the enthalpy of the sophorose binding to Bet v 1 may be too low to sufficiently counteract the loss in entropy resulting in a dissociation constant that cannot safely be determined with the applied experiments. In contrast, on Q3OS binding its sophorose moiety is forced into binding by the high affinity of the quercetin moiety and each additional protein–ligand contact co-operatively lowers the dissociation constant. Alternatively, the change in order of the solvent may simply be different for sophorose and Q3OS as compared with their Bet v 1 complexes [52]. A similar effect of glycosylation on affinities could be observed with the HIV protein gp120 and the human CD4 receptor [53]. Therefore we assume that the architecture of the binding pocket of Bet v 1a is specific for Q3OS and is optimized for carbohydrate binding.

The amino acids variable among the Bet v 1 isoforms are uniformly distributed among the sequences, however, many of these residues are spatially located in the peripheral region of the sophorose moiety given the prediction of the Q3OS binding geometry. This may be the structural basis for the observation that specificity for a certain ligand is isoform dependent [33].

Physiological relevance

The enzymatic activity of various allergenic proteins such as Der p 1 from house dust mite has been suggested to promote airway inflammation and therefore influence sensitization [54–56]. Although for Bet v 1a a transport or storage function without enzymatic activity has been proposed [21], its physiological function may nevertheless influence its allergenicity as ligands may induce unspecific inflammatory responses or will affect the immunological shift towards an allergic reaction [40]. Bet v 1–ligand interaction generally leads to an increase of the volume of the hydrophobic pocket [29,33], altering the protein surface and thus the IgE-binding epitopes. However, whether or not these structural changes influence allergenicity currently remains unanswered.

As the physiological ligand of Bet v 1 is a glycosylated flavonol, Bet v 1 may be linked with various activities in plants. Flavonoids contribute to the formation of pigments in flowering plants, they act as signals for pollinators, they are involved in plant hormone signalling, they facilitate pollen-tube germination and they protect plants from UV radiation [57,58]. Pollen from different plants, such as petunia, maize or *Ophrys*, have been studied, and flavonol glycosides with diverse flavonoid and sugar moieties identified [59,60]. At least ten glycosides of kaempferol, quercetin and isorhamnetin were found in maize pollen [61]. Interruption of kaempferol synthesis in petunia and maize resulted in self-sterile plants due to a failure in the production of functional pollen tubes. Even though flavonols in pollen only occur as sugar conjugates, pollen tube formation could be rescued by the artificial addition of flavonol aglycones. This indicates that the flavonoids are stored as glycosylated precursors and at some point, probably during rehydration of the pollen grain, are processed into their active form by pollen glycosyltransferases [57,59-63]. At this time point the lipid- or glycolipid-binding capability of Bet v 1 may lead to the displacement of Q3OS from the Bet v 1–Q3OS complex making Q3OS accessible for deglycosylation. Therefore Bet v 1 binding to lipids may not only play an important role in its uptake by nasal and conjunctival epithelial cells during allergic inflammatory response, but also be a physiological function as well [28,30,64,65]. Generally, the vast majority of pollen flavonoids are present as sugar-conjugated highly water-soluble flavonol-3-*O*-glycoside [61,66]. Synthesis of the flavonol is catalysed in the tapetal cells, and glycosylation is the final step after the non-polar molecule has entered the pollen grain [63,67–69].

Flavonoids like quercetin-3-*O*-glycosides are expressed upon UV-B radiation stress in petunia leaves (in contrast with, e.g. kaempferol-3-*O*-glycosides) [70], where they absorb UV radiation and have antioxidant capacities [58]. Thus Q3OS together with the high Bet v 1 content may be a means to protect birch pollen DNA from UV damage.

We thus hypothesize that after entering birch pollen quercetin is glycosylated into Q3OS to enhance its solubility. Bet v 1 stores Q3OS until pollen germination. The Bet v 1–Q3OS complex protects the birch pollen DNA from UV damage, and functional Q3OS may serve as an important signal for unharmed pollen DNA. On contact of the pollen with the stigma, glycosidase activity is induced and Q3OS is transformed into quercetin, which in turn enables the pollen to germinate. The known mixture of Bet v 1 isoforms in the pollen may match the diversity of flavonol glycosides, possibly providing an individual fingerprint preventing self-pollination.

AUTHOR CONTRIBUTION

Christian Seutter von Loetzen performed the UV/VIS and NMR titrations as well as the computational docking. Thomas Hoffmann and Wilfried Schwab identified Q3OS and isolated the compound from birch pollen. Maximilian Hartl designed the fluorescence measurements and performed them together with Christian Seutter von Loetzen and Olivia Hartl-Spiegelhauer. Kristian Schweimer and Christian Seutter von Loetzen conducted the STD measurements and NMR assignments. Olivia Hartl-Spiegelhauer performed the extraction of Bet v 1 from birch pollen and the reconstitution of Bet v 1a with Q3OS. Paul Rösch and Olivia Hartl-Spiegelhauer designed and supervised the project. Thomas Hoffmann, Wilfried Schwab, Paul Rösch, Maximilian Hartl and Olivia Hartl-Spiegelhauer wrote the paper, which was read and approved by all authors.

ACKNOWLEDGEMENTS

We thank Timo Stark (Food Chemistry and Molecular Sensory Science, Technische Universität München, Munich, Germany) for LC-TOF analysis, Ramona Heissmann (Lehrstuhl Biopolymere and Forschungszentrum für Bio-Makromoleküle, Universität Bayreuth, Bayreuth, Germany) for excellent technical assistance, and Professor Dr Bernd Meyer (Institute of Organic Chemistry and Institute of Biochemistry and Molecular Biology, University of Hamburg, Hamburg, Germany) for helpful discussions.

FUNDING

This work was supported by the Sonderforschungsbereich (SFB) [grant number 924 (to W.S.)].

© The Authors Journal compilation © 2014 Biochemical Society

REFERENCES

1 Ipsen, H. and Lowenstein, H. (1983) Isolation and immunochemical characterization of the major allergen of birch pollen (*betula verrucosa*). J. Allergy Clin. Immunol. **72**, 150–159
2 Schenk, M. F., Cordewener, J. H., America, A. H., Van't Westende, W. P., Smulders, M. J. and Gilissen, L. J. (2009) Characterization of PR-10 genes from eight betula species and detection of Bet v 1 isoforms in birch pollen. BMC Plant. Biol. **9**, 24
3 D'Amato, G., Spieksma, F. T., Liccardi, G., Jager, S., Russo, M., Kontou-Fili, K., Nikkels, H., Wuthrich, B. and Bonini, S. (1998) Pollen-related allergy in europe. Allergy **53**, 567–578
4 Wuthrich, B., Schindler, C., Leuenberger, P. and Ackermann-Liebrich, U. (1995) Prevalence of atopy and pollinosis in the adult population of switzerland (SAPALDIA study). Swiss study on air pollution and lung diseases in adults. Int. Arch. Allergy Immunol. **106**, 149–156
5 Vieths, S., Scheurer, S. and Ballmer-Weber, B. (2002) Current understanding of cross-reactivity of food allergens and pollen. Ann. N.Y. Acad. Sci. **964**, 47–68
6 Jarolim, E., Rumpold, H., Endler, A. T., Ebner, H., Breitenbach, M., Scheiner, O. and Kraft, D. (1989) IgE and IgG antibodies of patients with allergy to birch pollen as tools to define the allergen profile of *Betula verrucosa*. Allergy **44**, 385–395
7 Moverare, R., Westritschnig, K., Svensson, M., Hayek, B., Bende, M., Pauli, G., Sorva, R., Haahtela, T., Valenta, R. and Elfman, L. (2002) Different IgE reactivity profiles in birch pollen-sensitive patients from six european populations revealed by recombinant allergens: an imprint of local sensitization. Int. Arch. Allergy Immunol. **128**, 325–335
8 Dreborg, S. (1988) Food allergy in pollen-sensitive patients. Ann. Allergy. **61**, 41–46
9 Geroldinger-Simic, M., Zelniker, T., Aberer, W., Ebner, C., Egger, C., Greiderer, A., Prem, N., Lidholm, J., Ballmer-Weber, B., Vieths, S. and Bohle, B. (2011) Birch pollen-related food allergy: clinical aspects and the role of allergen-specific IgE and IgG4 antibodies. J. Allergy Clin. Immunol. **127**, 616–622
10 Liu, J. and Ekramoddoullah, A. K. M. (2006) The family 10 of plant pathogenesis-related proteins: their structure, regulation, and function in response to biotic and abiotic stresses. Physiol. Mol. Plant Pathol. **68**, 3–13
11 Breda, C., Sallaud, C., el-Turk, J., Buffard, D., de Kozak, I., Esnault, R. and Kondorosi, A. (1996) Defense reaction in medicago sativa: a gene encoding a class 10 PR protein is expressed in vascular bundles. Mol. Plant Microbe Interact. **9**, 713–719
12 Robert, N., Ferran, J., Breda, C., Coutos-Thévenot, P., Boulay, M., Buffard, D. and Esnault, R. (2001) Molecular characterization of the incompatible interaction of *Vitis vinifera* leaves with *Pseudomonas syringae* pv. *pisi*: expression of genes coding for stilbene synthase and class 10 PR protein. Eur. J. Plant Pathol. **107**, 249–261
13 Somssich, I. E., Schmelzer, E., Bollmann, J. and Hahlbrock, K. (1986) Rapid activation by fungal elicitor of genes encoding "pathogenesis-related" proteins in cultured parsley cells. Proc. Natl. Acad. Sci. U.S.A. **83**, 2427–2430
14 Walter, M. H., Liu, J. W., Grand, C., Lamb, C. J. and Hess, D. (1990) Bean pathogenesis-related (PR) proteins deduced from elicitor-induced transcripts are members of a ubiquitous new class of conserved PR proteins including pollen allergens. Mol. Gen. Genet. **222**, 353–360
15 Warner, S. A. J., Scott, R. and Draper, J. (1992) Characterisation of a wound-induced transcript from the monocot asparagus that shares similarity with a class of intracellular pathogenesis-related (PR) proteins. Plant Mol. Biol. **19**, 555–561
16 Walter, M. H., Liu, J. W., Wunn, J. and Hess, D. (1996) Bean ribonuclease-like pathogenesis-related protein genes (Ypr10) display complex patterns of developmental, dark-induced and exogenous-stimulus-dependent expression. Eur. J. Biochem. **239**, 281–293
17 Hoffmann-Sommergruber, K. (2000) Plant allergens and pathogenesis-related proteins. what do they have in common? Int. Arch. Allergy Immunol. **122**, 155–166
18 Ferreira, F. D., Hoffmann-Sommergruber, K., Breiteneder, H., Pettenburger, K., Ebner, C., Sommergruber, W., Steiner, R., Bohle, B., Sperr, W. R. and Valent, P. (1993) Purification and characterization of recombinant Bet v I, the major birch pollen allergen. immunological equivalence to natural Bet v I. J. Biol. Chem. **268**, 19574–19580
19 Swoboda, I., Jilek, A., Ferreira, F., Engel, E., Hoffmann-Sommergruber, K., Scheiner, O., Kraft, D., Breiteneder, H., Pittenauer, E. and Schmid, E. (1995) Isoforms of Bet v 1, the major birch pollen allergen, analyzed by liquid chromatography, mass spectrometry, and cDNA cloning. J. Biol. Chem. **270**, 2607–2613
20 Faber, C., Lindemann, A., Sticht, H., Ejchart, A., Kungl, A., Susani, M., Frank, R. W., Kraft, D., Breitenbach, M. and Rösch, P. (1996) Secondary structure and tertiary fold of the birch pollen allergen Bet v 1 in solution. J. Biol. Chem. **271**, 19243–19250
21 Gajhede, M., Osmark, P., Poulsen, F. M., Ipsen, H., Larsen, J. N., Joost van Neerven, R. J., Schou, C., Lowenstein, H. and Spangfort, M. D. (1996) X-ray and NMR structure of Bet v 1, the origin of birch pollen allergy. Nat. Struct. Biol. **3**, 1040–1045
22 Schweimer, K., Sticht, H., Nerkamp, J., Boehm, M., Breitenbach, M., Vieths, S. and Rösch, P. (1999) NMR spectroscopy reveals common structural features of the birch pollen allergen Bet v 1 and the cherry allergen Pru a 1. Appl. Magn. Reson. **17**, 449–456
23 Ferreira, F., Ebner, C., Kramer, B., Casari, G., Briza, P., Kungl, A. J., Grimm, R., Jahn-Schmid, B., Breiteneder, H., Kraft, D. et al. (1998) Modulation of IgE reactivity of allergens by site-directed mutagenesis: potential use of hypoallergenic variants for immunotherapy. FASEB J. **12**, 231–242
24 Krebitz, M., Wiedermann, U., Essl, D., Steinkellner, H., Wagner, B., Turpen, T. H., Ebner, C., Scheiner, O. and Breiteneder, H. (2000) Rapid production of the major birch pollen allergen Bet v 1 in *Nicotiana benthamiana* plants and its immunological *in vitro* and *in vivo* characterization. FASEB J. **14**, 1279–1288
25 Mirza, O., Henriksen, A., Ipsen, H., Larsen, J. N., Wissenbach, M., Spangfort, M. D. and Gajhede, M. (2000) Dominant epitopes and allergic cross-reactivity: complex formation between a fab fragment of a monoclonal murine IgG antibody and the major allergen from birch pollen Bet v 1. J. Immunol. **165**, 331–338
26 Spangfort, M. D., Mirza, O., Ipsen, H., Joost van Neerven, R. J., Gajhede, M. and Larsen, J. N. (2003) Dominating IgE-binding epitope of Bet v 1, the major allergen of birch pollen, characterized by X-ray crystallography and site-directed mutagenesis. J. Immunol. **171**, 3084–3090
27 Mittag, D., Batori, V., Neudecker, P., Wiche, R., Friis, E. P., Ballmer-Weber, B. K., Vieths, S. and Roggen, E. L. (2006) A novel approach for investigation of specific and cross-reactive IgE epitopes on Bet v 1 and homologous food allergens in individual patients. Mol. Immunol. **43**, 268–278
28 Mogensen, J. E., Wimmer, R., Larsen, J. N., Spangfort, M. D. and Otzen, D. E. (2002) The major birch allergen, Bet v 1, shows affinity for a broad spectrum of physiological ligands. J. Biol. Chem. **277**, 23684–23692
29 Markovic-Housley, Z., Degano, M., Lamba, D., von Roepenack-Lahaye, E., Clemens, S., Susani, M., Ferreira, F., Scheiner, O. and Breiteneder, H. (2003) Crystal structure of a hypoallergenic isoform of the major birch pollen allergen Bet v 1 and its likely biological function as a plant steroid carrier. J. Mol. Biol. **325**, 123–133
30 Mogensen, J. E., Ferreras, M., Wimmer, R., Petersen, S. V., Enghild, J. J. and Otzen, D. E. (2007) The major allergen from birch tree pollen, Bet v 1, binds and permeabilizes membranes. Biochemistry **46**, 3356–3365
31 Koistinen, K. M., Kokko, H. I., Hassinen, V. H., Tervahauta, A. I., Auriola, S. and Kärenlampi, S. O. (2002) Stress-related RNase PR-10c is post-translationally modified by glutathione in birch. Plant Cell Environ. **25**, 707–715
32 Koistinen, K. M., Soininen, P., Venalainen, T. A., Hayrinen, J., Laatikainen, R., Perakyla, M., Tervahauta, A. I. and Karenlampi, S. O. (2005) Birch PR-10c interacts with several biologically important ligands. Phytochemistry **66**, 2524–2533
33 Kofler, S., Asam, C., Eckhard, U., Wallner, M., Ferreira, F. and Brandstetter, H. (2012) Crystallographically mapped ligand binding differs in high and low IgE binding isoforms of birch pollen allergen Bet v 1. J. Mol. Biol. **422**, 109–123
34 Grote, M., Vrtala, S. and Valenta, R. (1993) Monitoring of two allergens, Bet v I and profilin, in dry and rehydrated birch pollen by immunogold electron microscopy and immunoblotting. J. Histochem. Cytochem. **41**, 745–750
35 Bollen, M. A., Garcia, A., Cordewener, J. H., Wichers, H. J., Helsper, J. P., Savelkoul, H. F. and van Boekel, M. A. (2007) Purification and characterization of natural bet v 1 from birch pollen and related allergens from carrot and celery. Mol. Nutr. Food Res. **51**, 1527–1536
36 Johnson, B. A. and Blevins, R. A. (1994) NMRview: a computer program for the visualization and analysis of NMR data. J. Biomol. NMR **4**, 603–614
37 Trott, O. and Olson, A. J. (2010) AutoDock vina: improving the speed and accuracy of docking with a new scoring function, efficient optimization, and multithreading. J. Comput. Chem. **31**, 455–461
38 Schüttelkopf, A. W. and van Aalten, D. M. (2004) PRODRG: a tool for high-throughput crystallography of protein-ligand complexes. Acta Crystallogr., Sect. D: Biol. Crystallogr. **60**, 1355–1363
39 Morris, G. M., Huey, R., Lindstrom, W., Sanner, M. F., Belew, R. K., Goodsell, D. S. and Olson, A. J. (2009) AutoDock4 and AutoDockTools4: automated docking with selective receptor flexibility. J. Comput. Chem. **30**, 2785–2791
40 Bufe, A. (1998) The biological function of allergens: relevant for the induction of allergic diseases? Int. Arch. Allergy Immunol. **117**, 215–219
41 Harborne, J. B., Baxter, H. and Moss, G. P. (1999) Phytochemical Dictionary: a Handbook of Bioactive Compounds From Plants, CRC Press, London
42 Ross, S. A., ElSohly, M. A., Sultana, G. N., Mehmedic, Z., Hossain, C. F. and Chandra, S. (2005) Flavonoid glycosides and cannabinoids from the pollen of cannabis sativa L. Phytochem. Anal. **16**, 45–48
43 Arraez-Roman, D., Zurek, G., Bässmann, C., Almaraz-Abarca, N., Quirantes, R., Segura-Carretero, A. and Fernandez-Gutierrez, A. (2007) Identification of phenolic compounds from pollen extracts using capillary electrophoresis-electrospray time-of-flight mass spectrometry. Anal. Bioanal. Chem. **389**, 1909–1917
44 Falkovskaia, E., Sengupta, P. K. and Kasha, M. (1998) Photophysical induction of dual fluorescence of quercetin and related hydroxyflavones upon intermolecular H-bonding to solvent matrix. Chem. Phys. Lett. **297**, 109–114

© The Authors Journal compilation © 2014 Biochemical Society

45 Ghiasi, M., Taheri, S. and Tafazzoli, M. (2010) Dynamic stereochemistry of rutin (vitamin P) in solution: theoretical approaches and experimental validation. Carbohydr. Res. **345**, 1760–1766
46 Bundle, D. R. and Young, N. M. (1992) Carbohydrate–protein interactions in antibodies and lectins. Curr. Opin. Struct. Biol. **2**, 666–673
47 Toone, E. J. (1994) Structure and energetics of protein-carbohydrate complexes. Curr. Opin. Struct. Biol. **4**, 719–728
48 García-Hernández, E., Zubillaga, R. A., Rojo-Domínguez, A., Rodríguez-Romero, A. and Hernández-Arana, A. (1997) New insights into the molecular basis of lectin-carbohydrate interactions: a calorimetric and structural study of the association of hevein to oligomers of N-acetylglucosamine. Proteins: Struct., Funct., Bioinf. **29**, 467–477
49 García-Hernández, E. and Hernández-Arana, A. (1999) Structural bases of lectin-carbohydrate affinities: comparison with protein-folding energetics. Protein Sci. **8**, 1075–1086
50 Dam, T. K. and Brewer, C. F. (2002) Thermodynamic studies of lectin–carbohydrate interactions by isothermal titration calorimetry. Chem. Rev. **102**, 387–430
51 Dunitz, J. D. (1995) Win some, lose some: enthalpy–entropy compensation in weak intermolecular interactions. Chem. Biol. **2**, 709–712
52 Holgersson, J., Gustafsson, A. and Breimer, M. E. (2005) Characteristics of protein–carbohydrate interactions as a basis for developing novel carbohydrate-based antirejection therapies. Immunol. Cell Biol. **83**, 694–708
53 Wilhelm, D., Behnken, H. N. and Meyer, B. (2012) Glycosylation assists binding of HIV protein gp120 to human CD4 receptor. ChemBioChem **13**, 524–527
54 Robinson, B. W., Venaille, T. J., Mendis, A. H. and McAleer, R. (1990) Allergens as proteases: an *Aspergillus fumigatus* proteinase directly induces human epithelial cell detachment. J. Allergy Clin. Immunol. **86**, 726–731
55 Herbert, C. A., King, C. M., Ring, P. C., Holgate, S. T., Stewart, G. A., Thompson, P. J. and Robinson, C. (1995) Augmentation of permeability in the bronchial epithelium by the house dust mite allergen der p1. Am. J. Respir. Cell Mol. Biol. **12**, 369–378
56 Hassim, Z., Maronese, S. E. and Kumar, R. K. (1998) Injury to murine airway epithelial cells by pollen enzymes. Thorax **53**, 368–371
57 Miller, K. D., Guyon, V., Evans, J. N., Shuttleworth, W. A. and Taylor, L. P. (1999) Purification, cloning, and heterologous expression of a catalytically efficient flavonol 3-O-galactosyltransferase expressed in the male gametophyte of petunia hybrida. J. Biol. Chem. **274**, 34011–34019
58 Brunetti, C., Di Ferdinando, M., Fini, A., Pollastri, S. and Tattini, M. (2013) Flavonoids as antioxidants and developmental regulators: relative significance in plants and humans. Int. J. Mol. Sci. **14**, 3540–3555
59 Karioti, A., Kitsaki, C. K., Zygouraki, S., Ziobora, M., Djeddi, S., Skaltsa, H. and Liakopoulos, G. (2008) Occurrence of flavonoids in ophrys (orchidaceae) flower parts. Flora **203**, 602–609
60 Mo, Y., Nagel, C. and Taylor, L. P. (1992) Biochemical complementation of chalcone synthase mutants defines a role for flavonols in functional pollen. Proc. Natl. Acad. Sci. U.S.A. **89**, 7213–7217
61 Ceska, O. and Styles, E. D. (1984) Flavonoids from *Zea mays* pollen. Phytochemistry **23**, 1822–1823
62 Taylor, L. P. and Miller, K. D. (2002) The use of a photoactivatable kaempferol analogue to probe the role of flavonol 3-O-galactosyltransferase in pollen germination. Adv. Exp. Med. Biol. **505**, 41–50
63 Vogt, T. and Taylor, L. P. (1995) Flavonol 3-O-glycosyltransferases associated with petunia pollen produce gametophyte-specific flavonol diglycosides. Plant Physiol. **108**, 903–911
64 Mattila, K. and Renkonen, R. (2009) Modelling of Bet v 1 binding to lipids. Scand. J. Immunol. **70**, 116–124
65 Golebski, K., Röschmann, K. I., Toppila-Salmi, S., Hammad, H., Lambrecht, B. N., Renkonen, R., Fokkens, W. J. and van Drunen, C. M. (2013) The multi-faceted role of allergen exposure to the local airway mucosa. Allergy **68**, 152–160
66 Strack, D., Meurer, B., Wray, V., Grotjahn, L., Austenfeld, F. A. and Wiermann, R. (1984) Quercetin 3-glucosylgalactoside from pollen of *Corylus avellana*. Phytochemistry **23**, 2970–2971
67 Xu, P., Vogt, T. and Taylor, L. P. (1997) Uptake and metabolism of flavonols during *in vitro* germination of *Petunia hybrida* (L.) pollen. Planta **202**, 257–265
68 Zerback, R., Bokel, M., Geiger, H. and Hess, D. (1989) A kaempferol 3-glucosylgalactoside and further flavonoids from pollen of petunia hybrida. Phytochemistry **28**, 897–899
69 Taylor, L. P. and Hepler, P. K. (1997) Pollen germination and tube growth. Annu. Rev. Plant Physiol. Plant Mol. Biol. **48**, 461–491
70 Ryan, K. G., Markham, K. R., Bloor, S. J., Bradley, J. M., Mitchell, K. A. and Jordan, B. R. (1998) UVB radiation induced increase in quercetin: kaempferol ratio in wild-type and transgenic lines of *Petunia*. Photochem. Photobiol. **68**, 323–330

Received 20 March 2013/25 October 2013; accepted 30 October 2013
Published as BJ Immediate Publication 30 October 2013, doi:10.1042/BJ20130413

© The Authors Journal compilation © 2014 Biochemical Society

Biochem. J. (2014) **457**, 379–390 (Printed in Great Britain) doi:10.1042/BJ20130413

online data

SUPPLEMENTARY ONLINE DATA

Secret of the major birch pollen allergen Bet v 1: identification of the physiological ligand

Christian SEUTTER VON LOETZEN*, Thomas HOFFMANN†, Maximilian J. HARTL*, Kristian SCHWEIMER*, Wilfried SCHWAB†, Paul RÖSCH* and Olivia HARTL-SPIEGELHAUER*[1]

*Lehrstuhl Biopolymere und Forschungszentrum für Bio-Makromoleküle, Universität Bayreuth, Universitätsstr. 30, 95447 Bayreuth, Germany
†Biotechnology of Natural Products, Technische Universität München, Liesel-Beckmann-Str. 1, 85354 Freising, Germany

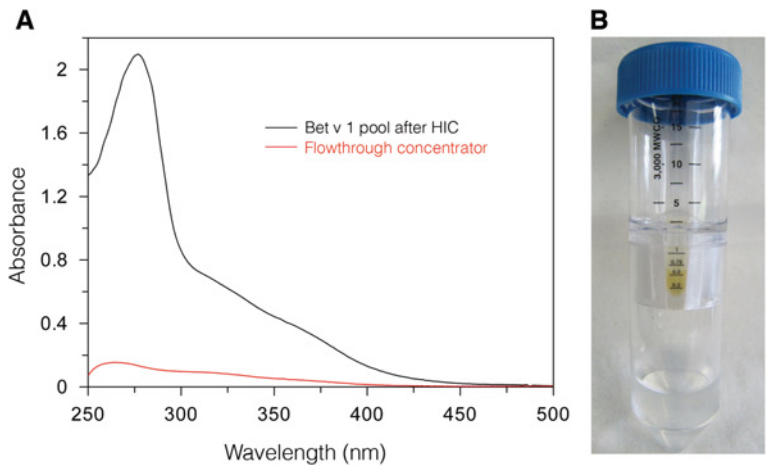


Figure S1 Concentration of isolated Bet v 1 fractions from mature birch pollen after hydrophobic interaction chromatography

(**A**) UV/VIS spectra of pooled Bet v 1 fractions after the hydrophobic interaction chromatography column, before concentration (black line) and the flow-through after concentration (red line). Conditions: 10 mM potassium phosphate buffer, pH 7.0, and ~1.5 M $(NH_4)_2SO_4$. Absorption spectra were recorded using an Agilent 8453 UV-visible spectrophotometer. (**B**) Picture of the concentrator (VIVASPIN 20 concentrator, molecular-mass cut-off 3000 Da, Sartorius Stedim Biotech) after concentration.

[1] To whom correspondence should be addressed (email Olivia.Hartl-Spiegelhauer@uni-bayreuth.de).

© The Authors Journal compilation © 2014 Biochemical Society

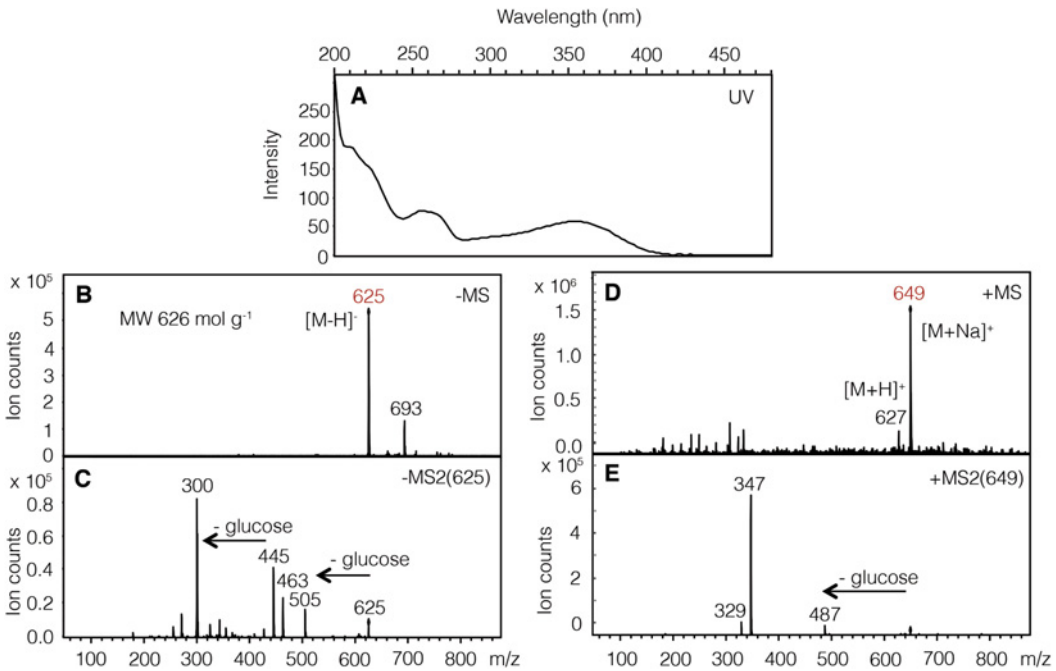


Figure S2 LC-DAD-MS analysis of Q3OS

UV maxima at 252 and 358 nm were determined (**A**). Pseudomolecular ions $[M-H]^-$ (**B**) and $[M+Na]^+$ (**D**) were observed in the negative and positive mode respectively. Product ion spectra of *m/z* 625 (**C**) and 649 (**E**) show the loss of two and one glucose residues respectively.

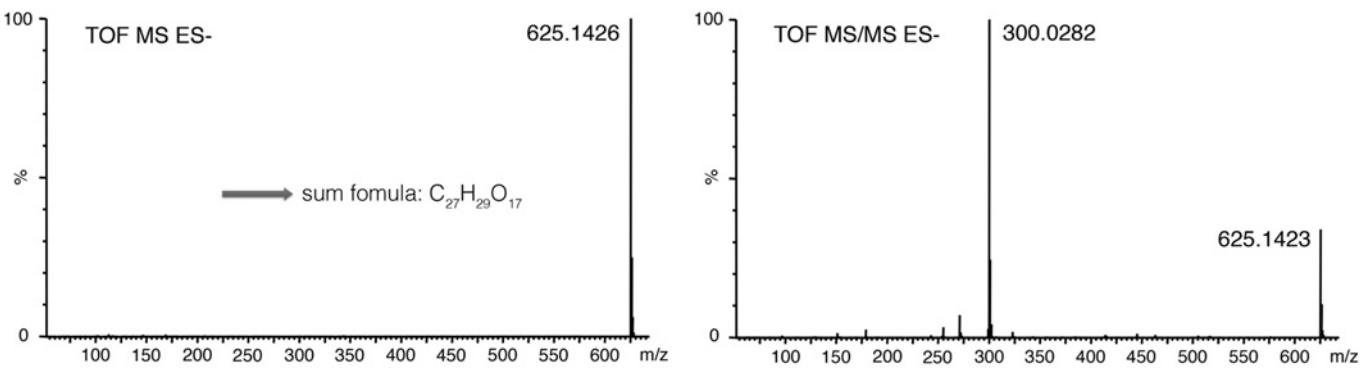


Figure S3 LC-TOF mass spectrum and MS^2 of Q3OS

LC-TOF mass spectrum (left-hand panel) and MS^2 (right-hand panel) of Q3OS. Spectra were acquired in the negative mode.

© The Authors Journal compilation © 2014 Biochemical Society

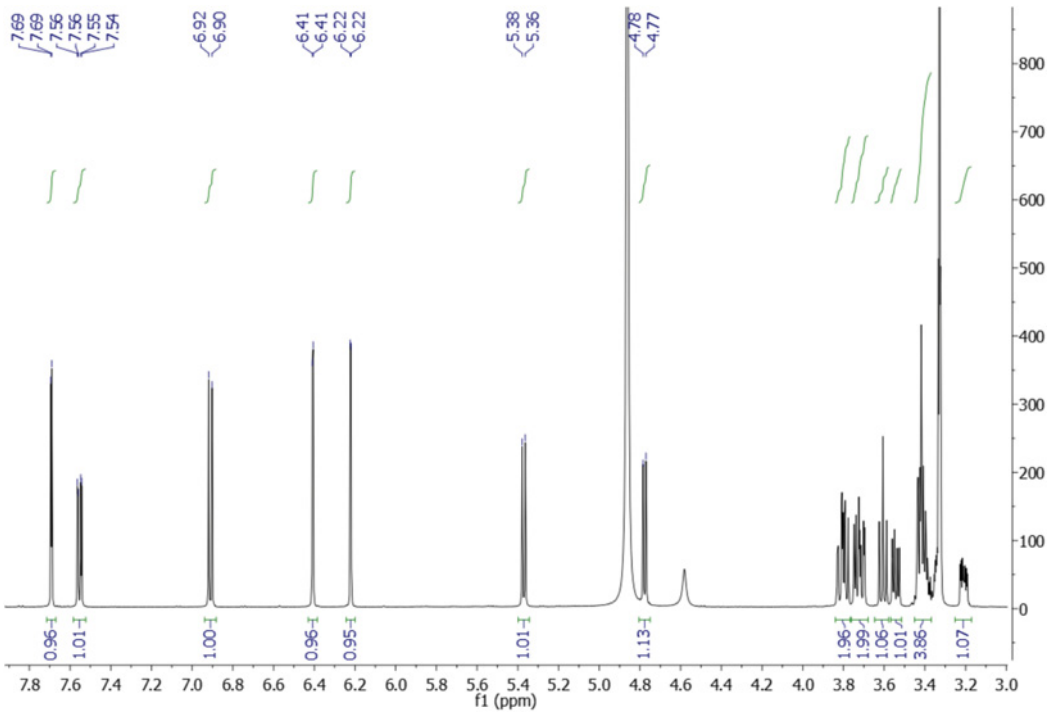


Figure S4 ^{1}H-NMR spectrum of Q3OS

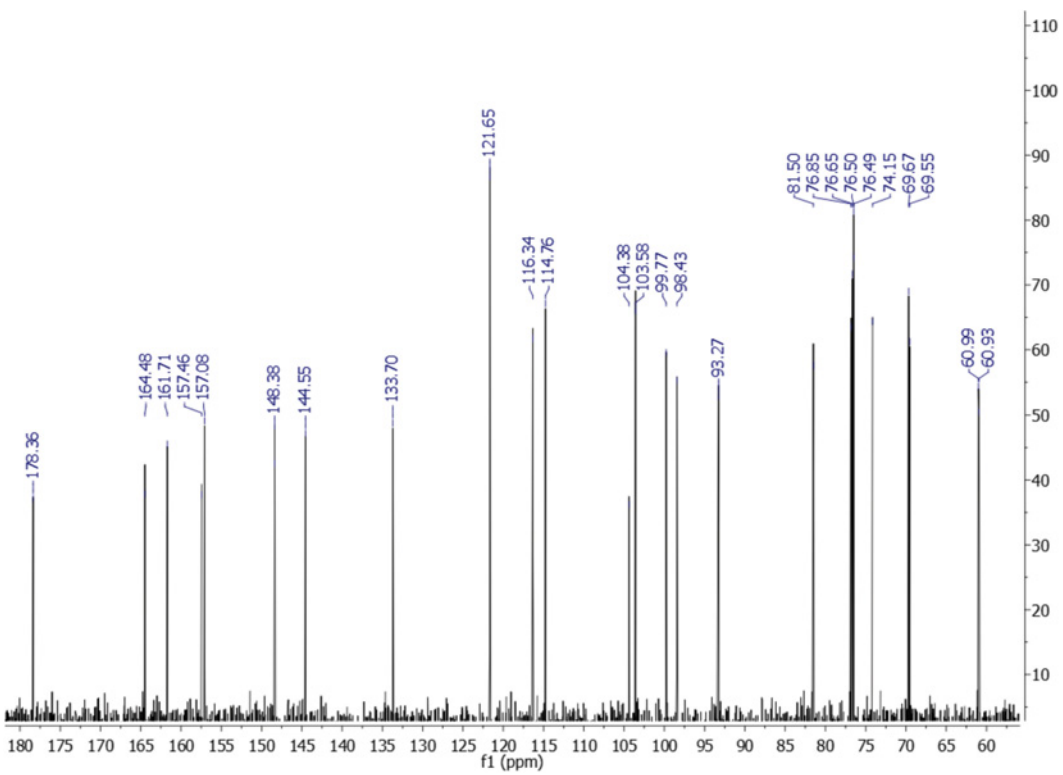


Figure S5 ^{13}C-NMR spectrum of Q3OS

© The Authors Journal compilation © 2014 Biochemical Society

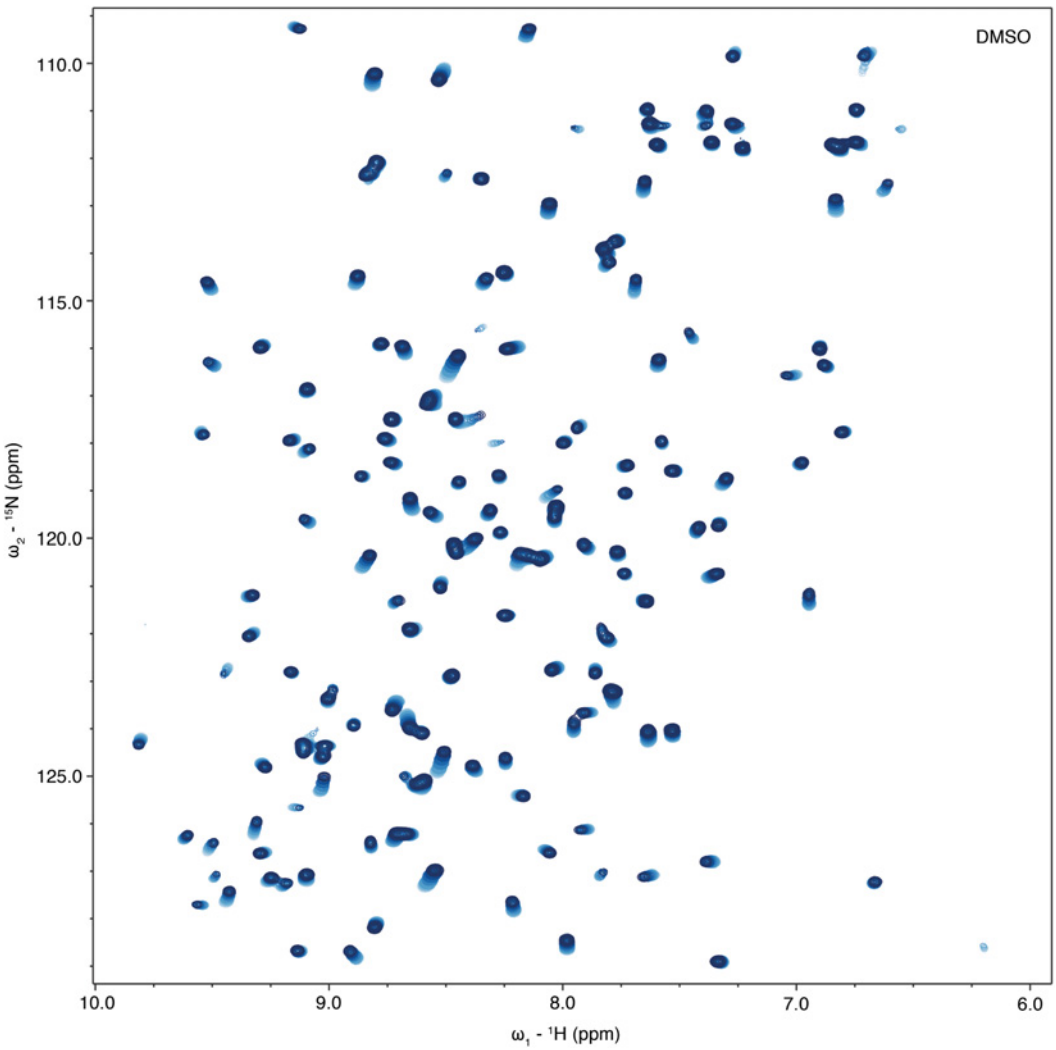


Figure S6 Overlay of eight ^{1}H-^{15}N HSQC spectra of ^{15}N-labelled Bet v 1a at increasing DMSO concentrations shown from light to dark blue

Bet v 1a (100 μM) was stepwise titrated with deuterated DMSO to a final concentration of 8.3 %. The experiment was performed in 50 mM sodium phosphate buffer, pH 7.0, 50 mM NaCl and 10 % $^{2}H_2O$ at 298 K.

© The Authors Journal compilation © 2014 Biochemical Society

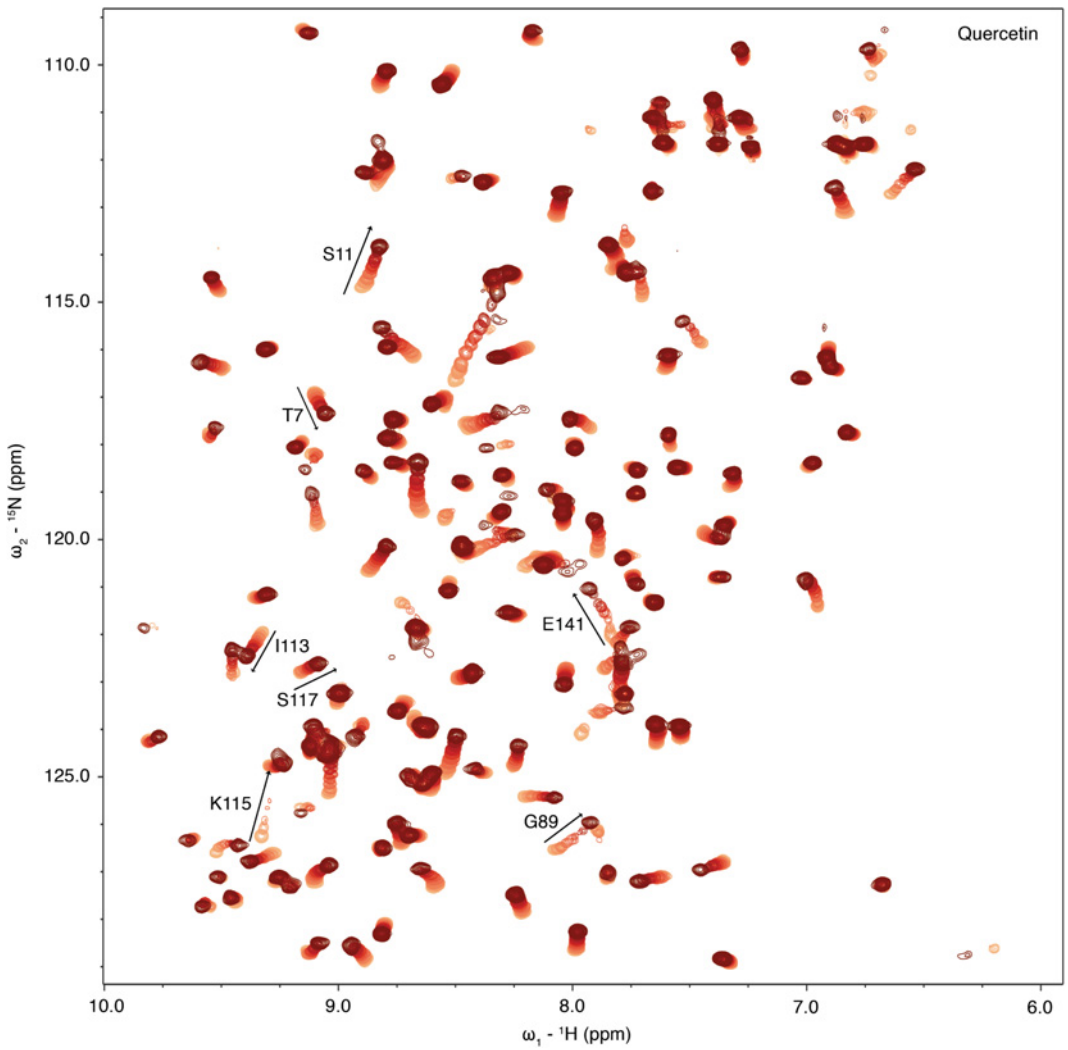


Figure S7 Overlay of ten ^{1}H-^{15}N HSQC spectra of ^{15}N-labelled Bet v 1a at increasing quercetin concentrations shown from light to dark red

Bet v 1a (100 μM) was stepwise titrated with a quercetin stock solution prepared in deuterated DMSO to a final excess of 1:15 over Bet v 1a and final a DMSO concentration of 13.5 % (v/v). The arrows indicate the residues, which were not influenced by the increasing DMSO concentrations and thus were used for K_d determination. The experiment was performed in 50 mM sodium phosphate buffer, pH 7.0, 50 mM NaCl and 10 % $^{2}H_2O$ at 298 K.

© The Authors Journal compilation © 2014 Biochemical Society

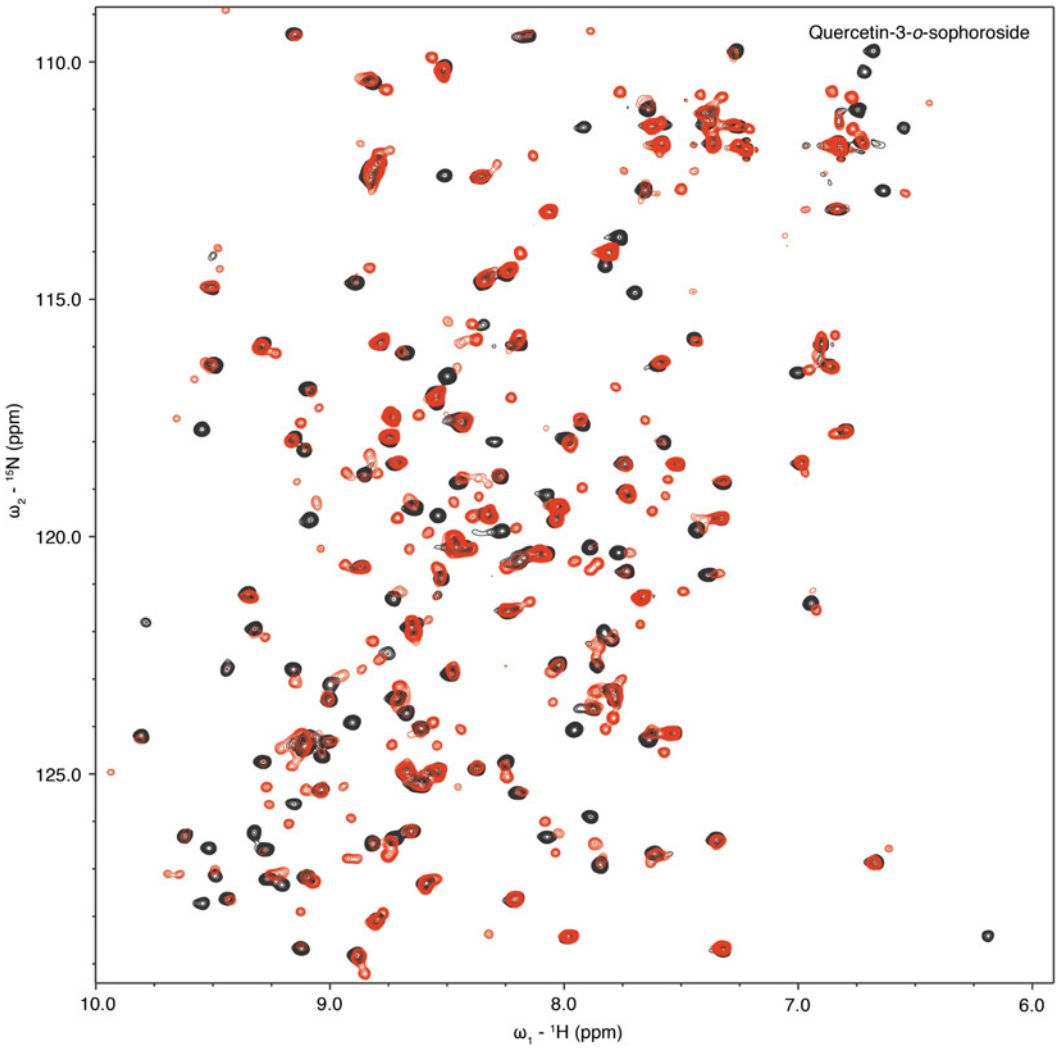


Figure S8 Overlay of two ^{1}H-^{15}N HSQC spectra of ^{15}N-labelled Bet v 1a in the absence (black) and presence (red) of a 15-fold excess of Q3OS

The experiment was performed in 50 mM sodium phosphate buffer, pH 7.0, 50 mM NaCl and 10 % $^{2}H_2O$ at 298 K.

© The Authors Journal compilation © 2014 Biochemical Society

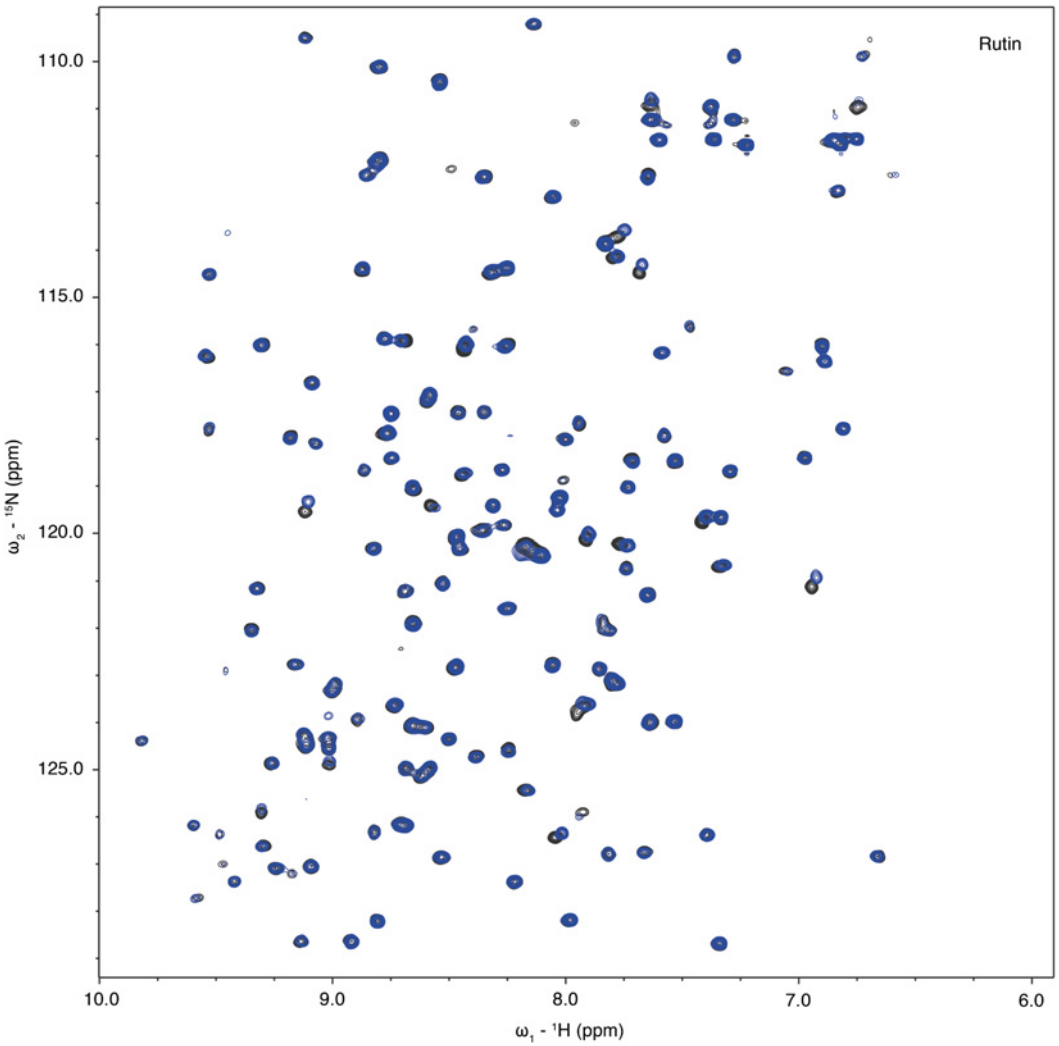


Figure S9 Overlay of two ^{1}H-^{15}N HSQC spectra of ^{15}N-labelled Bet v 1a in the absence (black) and presence (blue) of a 15-fold excess of rutin

Rutin was added from a stock solution prepared in DMSO resulting in a final DMSO concentration of 10 % (v/v). The experiment was performed in 50 mM sodium phosphate buffer, pH 7.0, 50 mM NaCl and 10 % $^{2}H_2O$ at 298 K.

© The Authors Journal compilation © 2014 Biochemical Society

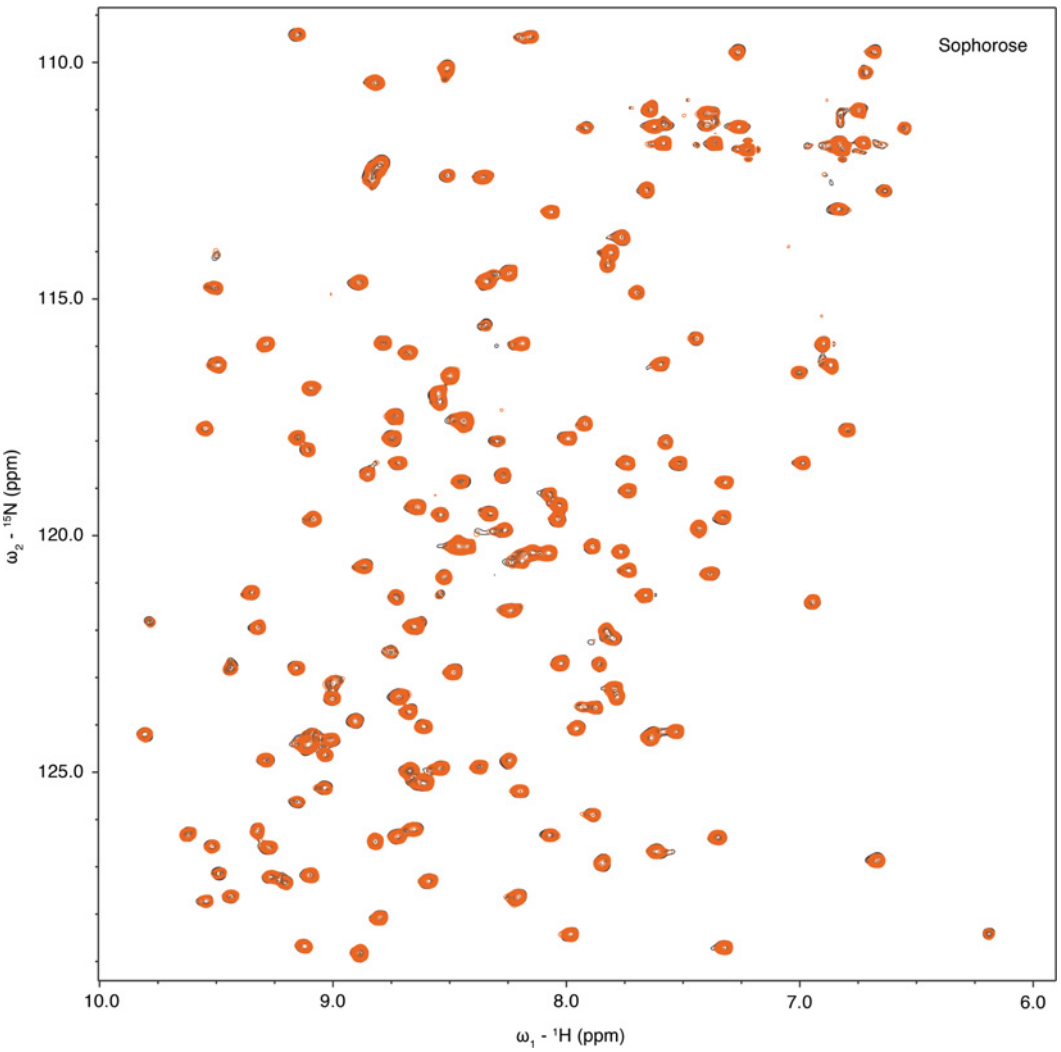


Figure S10 Overlay of two ^{1}H-^{15}N HSQC spectra of ^{15}N-labelled Bet v 1a in the absence (black) and presence (orange) of a 15-fold excess of sophorose

The experiment was performed in 50 mM sodium phosphate buffer, pH 7.0, 50 mM NaCl and 10 % $^{2}H_2O$ at 298 K.

© The Authors Journal compilation © 2014 Biochemical Society

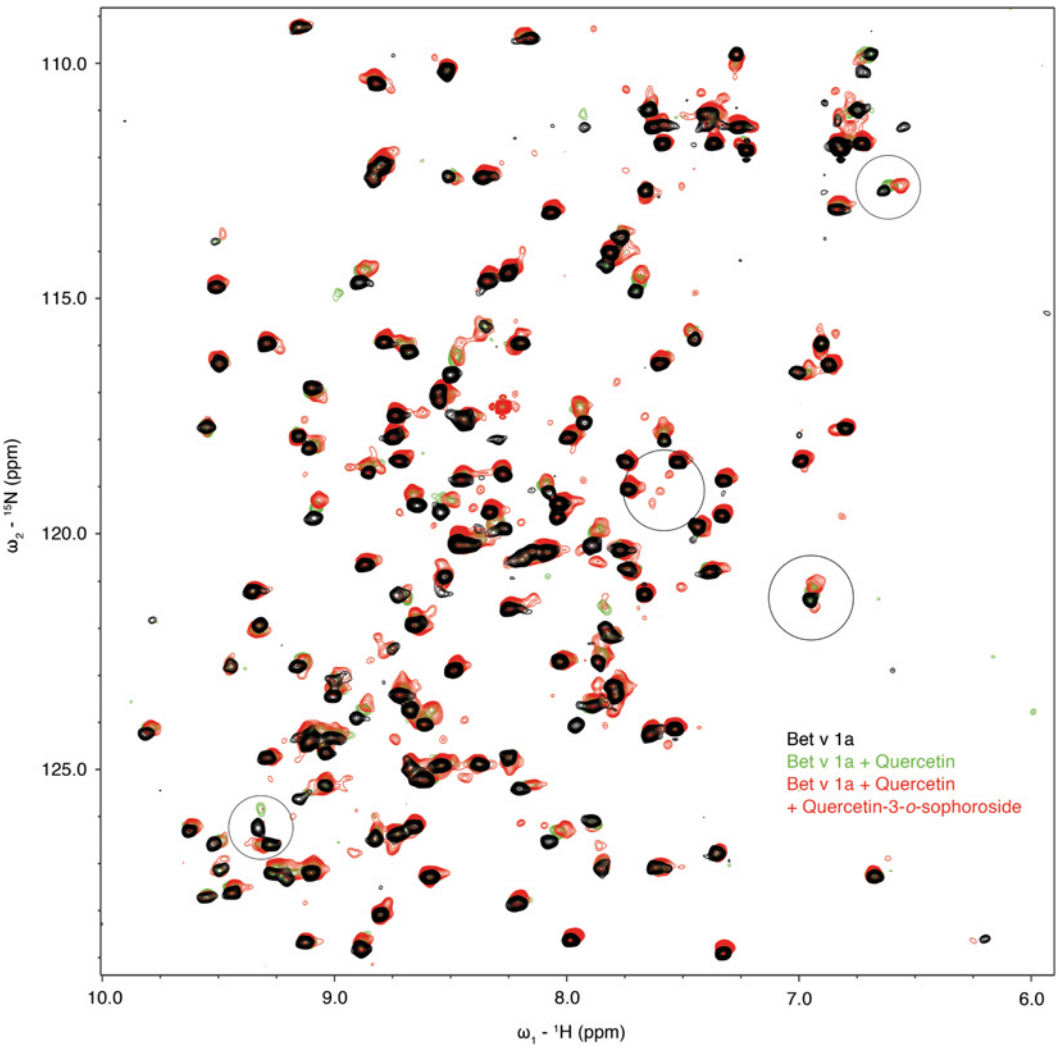


Figure S11 Displacement of quercetin bound to Bet v 1a by Q3OS

Overlay of three ^{1}H-^{15}N HSQC spectra of 100 μM ^{15}N-labelled Bet v 1a (black), 100 μM ^{15}N-labelled Bet v 1a + 25 μM quercetin (green) and 100 μM ^{15}N-labelled Bet v 1a + 25 μM quercetin + 1 mM Q3OS. The circles highlight regions in which the replacement can be seen clearly. The experiment was performed in 50 mM sodium phosphate buffer, pH 7.0, 50 mM NaCl and 10 % $^{2}H_2O$ at 298 K.

© The Authors Journal compilation © 2014 Biochemical Society

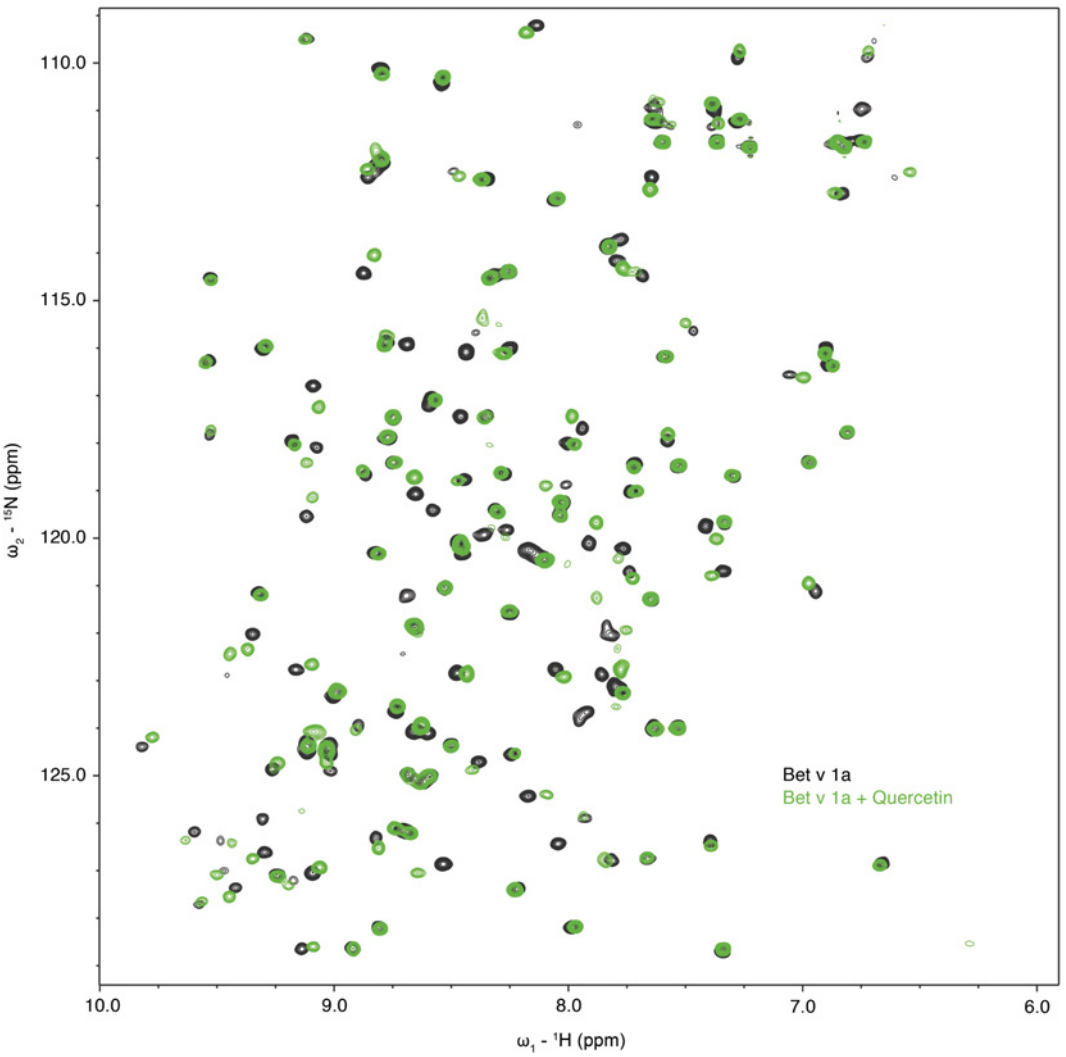


Figure S12 Overlay of two ^{1}H-^{15}N HSQC spectra of ^{15}N-labelled Bet v 1a in 10 % (v/v) DMSO in the absence (black) and presence (green) of a 15-fold excess of quercetin

Quercetin was added from a stock solution prepared in DMSO resulting in an unchanged DMSO concentration of 10 % (v/v). The experiment was performed in 50 mM sodium phosphate buffer, pH 7.0, 50 mM NaCl and 10 % $^{2}H_2O$ at 298 K.

© The Authors Journal compilation © 2014 Biochemical Society

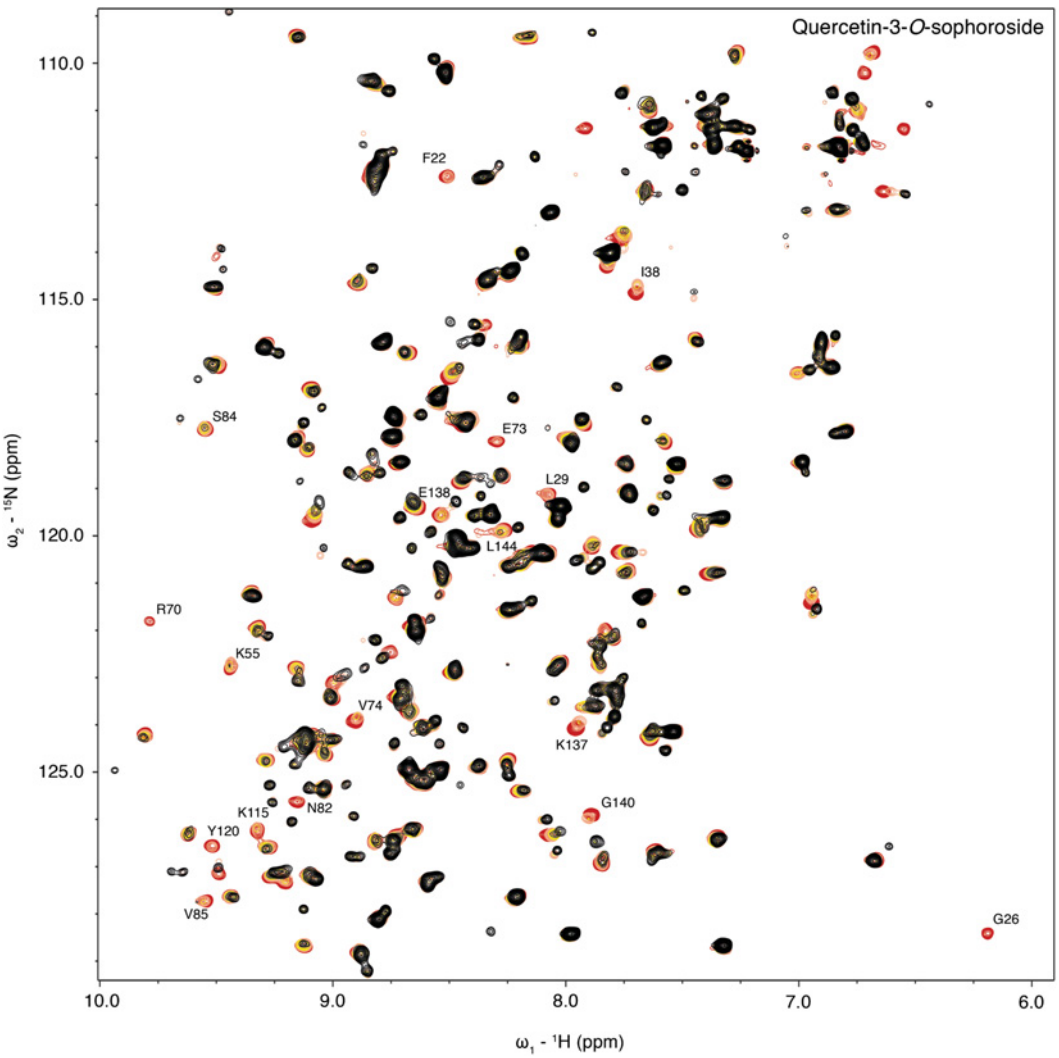
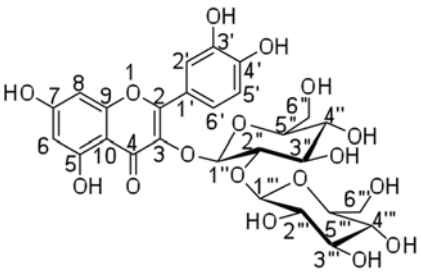


Figure S13 Effect of Q3OS on the ^{1}H-^{15}N chemical shifts of ^{15}N-labelled Bet v 1a (red)

The protein was added stepwise to 680 μM Q3OS in ratios (Q3OS/Bet v 1a) of 15:1 (black), 10:1 (grey), 5:1 (yellow) and 2.4:1 (light red). Labelled residues indicate those with disappearing signals. The experiment was performed in 50 mM sodium phosphate buffer, pH 7.0, 50 mM NaCl and 10 % $^{2}H_2O$ at 298 K.

© The Authors Journal compilation © 2014 Biochemical Society

Table S1 ^{1}H- and ^{13}C-NMR data of Q3OS

Atom Reference	^{13}C [1]	^{1}H [1]	^{13}C [2]	^{1}H [2]	^{13}C [3]	^{13}C The present study	^{1}H The present study
							
2	156.7				154.98	157.5	
3	133.5				132.45	133.7	
4	177.9				176.90	178.4	
5	161.6				160.72	161.7	
6	98.5	6.17 d (2.4)	98.9	6.18 d (2.1)	97.98	98.4	6.22 d (2.1)
7	164.4				163.45	164.5	
8	93.8	6.39 d (1.8)	93.7	6.41 d (1.5)	92.87	93.3	6.41 d (2.1)
9	156.0				155.68	157.1	
10	104.5				103.39	104.4	
1′	122.2				120.58	121.7	
2′	116.5	7.56 d (2.3)	115.6	7.55 d (2.4)	115.51	116.4	7.69 d (2.2)
3′	145.1				144.27	144.6	
4′	148.8				147.95	148.4	
5′	115.8	6.87 d (7.8)	116.2	6.87 d (8.5)	115.27	114.8	6.91 d (8.4)
6′	121.6	7.45 m	122.0	7.60 dd (2.1;8.5)	121.30	121.7	7.55 dd (2.2;8.4)
Sugar at C^{3}							
1″	99.0	5.67 d (7.2)	98.2	5.69 d (7.0)	97.45	99.8	5.37 d (7.5)
2″	83.1	3.52 t (8.4)	82.9		82.20	81.5	
3″	76.9	3.49 t (8.4)	76.8		75.99	76.5	
4″	69.9	3.15 t (8.4)	69.7		69.39	69.7	
5″	77.8	3.08 m	77.7		76.98	76.9	
6″	61.0	3.28 m	60.8		60.08	61.0	
		3.29 dd (6.0; 12.0)					
Sugar at C$^{2''}$							
1‴	104.4	4.60 d (7.2)	104.4	4.60 d (7.9)	103.66	103.6	4.78 d (7.2)
2‴	74.6	3.17 t (8.4)	74.6		73.85	74.2	
3‴	76.8	3.20 t (8.4)	76.7		75.99	76.5	
4‴	69.8	3.10 t (8.4)	69.7		69.04	69.6	
5‴	77.1	3.14 m	77.0		75.99	76.7	
6‴	60.9	3.54 m	60.8		60.14	60.9	
		3.47 m					

REFERENCES

1 Nørbaek, R. and Kondo, T. (1999) Flavonol glycosides from flowers of *Crocus speciosus* and *C. antalyensis*. Phytochemistry **51**, 1113–1119

2 Gluchoff-Fiasson, K., Fiasson, J. L. and Waton, H. (1997) Quercetin glycosides from European aquatic *Ranunculus* species of subgenus *Batrachium*. Phytochemistry **45**, 1063–1067

3 Price, K. R., Casuscelli, F., Colquhoun, I. J. and Rhodes, M. J. C. (1998) Composition and content of flavonol glycosides in broccoli florets (*Brassica olearacea*) and their fate during cooking. J. Sci. Food Agric. **77**, 468–472

Received 20 March 2013/25 October 2013; accepted 30 October 2013
Published as BJ Immediate Publication 30 October 2013, doi:10.1042/BJ20130413

© The Authors Journal compilation © 2014 Biochemical Society